Published in final edited form as:
Mar Pollut Bull. 2009 ; 59(4-7): 193–206. doi:10.1016/j.marpolbul.2009.02.022.

Bivalves as indicators of environmental variation and potential anthropogenic impacts in the southern Barents Sea

Michael L. Carroll[1,*], **Beverly J. Johnson**[2], **Gregory A. Henkes**[2,3,†], **Kelton W. McMahon**[4], **Andrey Voronkov**[5,6], **William G. Ambrose Jr.**[1,3], and **Stanislav G. Denisenko**[5]

[1] Akvaplan-niva, Polar Environmental Centre, N-9296 Tromsø, Norway

[2] Bates College, Department of Geology, Lewiston, Maine 04240, USA

[3] Bates College, Department of Biology, Lewiston, Maine 04240, USA

[4] Woods Hole Oceanographic Institution, MIT-WHOI Joint Program in Biological, Oceanography, Woods Hole, MA 02543-1541 USA

[5] Zoological Institute, Russian Academy of Sciences, Universitetskaya nab. 1, St. Petersburg, 199034, Russia

[6] Norwegian Polar Institute, Polar Environmental Centre, N-9296 Tromsø, Norway

Abstract

Identifying patterns and drivers of natural variability in populations is necessary to gauge potential effects of climatic change and the expected increases in commercial activities in the Arctic on communities and ecosystems. We analyzed growth rates and shell geochemistry of the circumpolar Greenland smooth cockle, *Serripes groenlandicus*, from the southern Barents Sea over almost 70 years between 1882 and 1968. The datasets were calibrated via annually-deposited growth lines, and growth, stable isotope ($\delta^{18}O$, $\delta^{13}C$), and trace elemental (Mg, Sr, Ba, Mn) patterns were linked to environmental variations on weekly to decadal scales. Standardized growth indices revealed an oscillatory growth pattern with a multi-year periodicity, which was inversely related to the North Atlantic Oscillation Index (NAO), and positively related to local river discharge. Up to 60% of the annual variability in the Ba/Ca could be explained by variations in river discharge at the site closest to the rivers, but the relationship disappeared at a more distant location. Patterns of $\delta^{18}O$, $\delta^{13}C$, and Sr/Ca together provide evidence that bivalve growth ceases at elevated temperatures during the fall and recommences at the coldest temperatures in the early spring, with the implication that food, rather than temperature, is the primary driver of bivalve growth. The multi-proxy approach of combining the annually integrated information from the growth results and higher resolution geochemical results yielded a robust interpretation of biophysical coupling in the region over temporal and spatial scales. We thus demonstrate that sclerochronological proxies can be useful retrospective analytical tools for establishing a baseline of ecosystem variability in assessing potential combined impacts of climatic change and increasing commercial activities on Arctic communities.

* Corresponding Author: M.L. Carroll, Tel: +47 7775 0318, Fax: +47 7775 0301, Email: E-mail: mc@akvaplan.niva.no.
†Current Address: Smithsonian Institution, Museum Conservation Institute, 4210 Silver Hill Road, MRC 534, Suitland, MD 20746-2863, USA

Keywords

Arctic; Barents Sea; benthic community; bivalve growth; climate oscillation; environmental forcing; North Atlantic Oscillation; White Sea; sclerochronology; *Serripes groenlandicus*; shell geochemistry; stable isotopes; trace element ratios

1. Introduction

The Arctic is warming and consequently becoming more accessible to industrial and commercial activities such as petroleum and mineral extraction, shipping, and fisheries (ACIA, 2005). As these activities increase, pre-industrial baselines of the natural system are necessary in order to assess the effects of anthropogenic activities on the Arctic marine ecosystem. This necessitates observations and data collections over time scales that capture the seasonal to decadal scales of system processes. Unfortunately, due to the remote setting and harsh nature of much of the Arctic marine ecosystem, relevant scales of observation are rarely adequate with traditional marine biological sampling plans, which usually provide a spatially- and temporally-limited view of the system. While continuously-recording observatories are a promising development (e.g. Morison et al., 2002), they are still in their infancy in the Arctic and currently provide data for limited locations. Biological proxies may provide an immediate alternative approach for assessing the variability of marine ecosystems over longer time frames, including the ability for retrospective reconstruction of environmental variability over historical time frames. Marine bivalves (clams) show great promise for investigating environmental variability in the Arctic. Arctic bivalves are long-lived (decades to centuries), sessile, and often dominate the biomass of many Arctic benthic communities (Zenkevich, 1963; McDonald et al., 1981; Dayton, 1990; Feder et al., 1994). Since bivalve growth is strongly regulated by temperature and food availability (Beukema et al., 1985; Jones et al., 1989; Lewis and Cerrato, 1997; Decker and Beukema, 1999), analyzing variations in growth can provide insight into seasonal to decadal variations in these factors over the animal's life.

Reconstructing environmental conditions from animal soft tissues offers a limited view of the past because of the rapid turnover rates of these highly metabolically-active tissues. Aragonitic bivalve shells, however, are secreted sequentially with external growth lines as the animal grows (Rhoads and Lutz, 1980), recording the growth histories, metabolism and environmental conditions experienced during the deposition of that shell material. The growth and chemistry of accretionary hard-parts precipitated by marine organisms have proved valuable in developing histories of environmental change in marine systems (Pannella, 1971; Andrews, 1972, 1973; Rhoads and Lutz, 1980; Jones, 1981; Weidman et al., 1994; Witbaard et al., 1999; Ambrose et al., 2006; reviewed in Richardson, 2001). High-latitude bivalves have provided uninterrupted long-term records of hydrographic conditions experienced during the lifetime of the organism (Thompson et al., 1980; Witbaard et al., 1999; Dutton et al., 2002; Müller-Lupp and Bauch, 2005).

The shell material of bivalves preserves chemical proxies for ambient seawater conditions when the organism is actively precipitating shell carbonate. Profiles of stable oxygen and carbon isotopes (Jones and Quitmyer, 1996; Klein et al., 1996; Müller-Lupp and Bauch, 2005; Simstich et al., 2005) and incorporated trace elements (Torres et al., 2001; Vander Putten et al., 2000; Khim et al., 2003; Freitas et al., 2006; Gillikin et al., 2006a) from sequential sampling along the shell height can provide high-resolution records of seawater chemistry useful for interpreting spatial and temporal patterns in temperature, salinity, and hydrography. External growth lines on bivalve shells often represent annual growth checks, as has been demonstrated for *Serripes groenlandicus* (Khim, 2002; Khim et al., 2003; Ambrose et al., 2006; Kilada et al., 2007). Provided the date of death is known, growth lines can be used to

determine growth rates and assign calendar years to geochemical proxies. The combined use of growth rate and shell geochemistry allows us to compare proxy information on specific environmental parameters and their biological manifestation, thereby allowing broader inferences on mechanistic relationships of bio-physical coupling.

The Barents Sea, a continental shelf sea bounded by Norway and Russia to the south and the Arctic Ocean basin to the north, is both bathymetrically and hydrographically complex (Loeng, 1991; Vinje and Kvambekk, 1991). The northern and eastern regions are dominated by Arctic water with origins in the Arctic Ocean and Russian shelf seas. The southern region is strongly influenced by warm, saline Atlantic source water from temperate latitudes. The coastal areas of the southern Barents Sea are under the influence of the eastern-flowing Murman Coastal Current as well as freshwater discharges from the Mezen', Severnaya Dvina, and Pechora Rivers (Loeng 1989, 1991; Loeng et al., 1997). These oceanographic regions and their hydrographic properties have strong influences on regional and local primary production and ecosystem structure (Wassmann et al., 2006), including benthic community structure (Carroll et al., 2008a) and functioning (Renaud et al., 2008). The overriding influence of these oceanographic provinces on properties of marine ecosystems is modified by regional climatic drivers which oscillate between different phases and are accompanied by substantially different atmospheric and hydrograhic properties over decadal scales. The North Atlantic Oscillation Index (NAO), usually defined as the atmospheric pressure difference between Iceland and Gibraltar, is one of the major modes of variability in the atmosphere of the Northern Hemisphere, (Jones et al., 1997; Osborn et al., 1999), and has been linked to weather patterns and concomitant ecosystem variability throughout Europe (e.g. Ottersen et. al., 2001).

Bivalve populations exhibit growth rates that vary with water masses in the Barents Sea (Tallqvist and Sundet, 2000; Carroll et al., 2008b, Carroll et al., submitted) and bivalves in the seasonally ice covered northern Barents Sea and Svalbard have been shown to be reflective of both large scale climatic forcing and more localized environmental conditions (Ambrose et al., 2006; Carroll et al., submitted). Climate variability in the Barents Sea has caused decadal-scale changes in the recruitment and productivity of commercially important fisheries and in the diversity and biomass of macrobenthic communities (Blacker, 1957, 1965; Denisenko et al., 1995; Sakshaug, 1997; Ottersen and Stenseth, 2001; Stenseth et al., 2004; Beuchel et al., 2006; Drinkwater, 2006). Detection of these climatic changes over long time scales is a necessary prerequisite to identifying scales of variability and thus assessing more direct anthropogenic effects related to local commercial activities.

We developed a long-term sclerochronological record of environmental change using the Greenland Smooth Cockle (*Serripes groenlandicus*) as an Arctic biological proxy. To do this, we investigated the variability of growth histories, stable isotopes ($\delta^{18}O$ and $\delta^{13}C$), and trace elements (Mg, Sr, Ba, Mn) in archived *S. groenlandicus* shells from the southern Barents Sea near the entrance to the White Sea collected over a period of almost 70 years. By analyzing interannual patterns of growth and trends in stable isotope and trace element ratios from different time periods, we demonstrate the use of bivalves as proxies leading to a better understanding of the range of variability in these Arctic systems over multiple temporal scales. This information will provide essential information about ecosystem function in this present era of climate change and increasing commercial activities in the Arctic.

2. Materials and Methods

2.1. Sample Collection

The Greenland Smooth Cockle (*Serripes groenlandicus*, hereafter referred to as ‘cockles’) is a circumpolar bivalve with a maximum size of about 100 mm and age of about 30 years (Kilada et al., 2007). The Laboratory of Marine Research, Zoological Institute of the Russian Academy

of Sciences, St. Petersburg (LMR-ZIN) maintains extensive collections of biological materials collected during Russian Arctic expeditions well into the 19th century. We made searches of the LMR-ZIN collections from original hand-written expedition logs of Arctic past expeditions in order to identify samples of cockles from the Barents Sea-Svalbard region. Specimens were then examined to make sure they met criterion making them suitable for analyses in the present project (e.g. precise collection coordinates, the presence of whole animals as well as shells indicating live collection, shells intact).

From this visual inspection, roughly 100 individuals were identified as potentially appropriate for use in the project. These individuals were further culled based on the time and location of collection, the size of individuals, and the visibility of growth lines on the shell. This resulted in a final sample population of 15 individuals from the southern Barents Sea in proximity to the entrance to the White Sea (Fig. 1), collected on expeditions between 1899 and 1968 (Table 1). These individuals covered the time period between 1882 and 1968, excluding only 1900-1904 and 1928-1943 (Table 1, Fig. 2). Here, we present growth data from all 15 of our shells, and geochemical data from two of the 15 shells.

2.2. Growth Rates

Each annual increment was measured externally as the linear length from the umbo to each successive dark growth line along the axis of greatest shell height toward the ventral shell margin. Since individuals were collected in the middle of a growth year, the last increment (outermost growth beyond the last dark growth line) was incomplete, and therefore excluded from further analyses. Measurements were made with MapViewer software from high resolution photographs and corroborated with caliper-based measurements of the total shell height. Cockles were collected live, so each growth increment can be assigned to a specific calendar year by counting sequentially back from the year of collection.

Bivalve growth declines with age, so raw growth increments within an individual and among individuals of different ages must be standardized before growth can be compared among years. We used the methods of Jones et al. (1989), employing the von Bertalanffy growth function with respect to time, to derive an ontogenetically-adjusted measure of annual growth (see Ambrose et al. (2006) and Carroll et al. (submitted) for a complete description of the application of the von Bertalanffy function to cockle populations).

After determining the average yearly changes in shell height based on growth data from all cockles in the sample population, we calculated the expected yearly increase in shell height for each cockle for each year. We then divided the measured yearly shell growth by the expected growth for that year to generate a Standardized Growth Index (SGI). This removed ontogenetic changes in growth and equalized the variance for the entire growth series (Fritts, 1976). The result is a record of year-by-year growth for the population. An SGI greater than 1.0 indicates a better than expected year of growth, while a value less than 1.0 reflects less than expected growth for that year. The growth rate of individuals at each station was determined by comparing growth curves (age at shell height) for each station. This was done by generating omega (ω) values for each individual at each station. The omega value is a single growth parameter derived from the von Bertalanffy growth function (Jones et al., 1989):

$$\omega = SH_{\infty} * k$$

where SH_{∞} = maximum asymptotic shell height and k = growth constant. This parameter corresponds to the growth rate near t_0 and is suitable for comparisons of organism growth-

functions between regions (Gallucci and Quinn, 1979; Appledoorn 1980, 1983; Jones et al., 1989).

2.3. Geochemical Analyses

2.3.1. Sample Preparation—Two archived shells (collection numbers 156 – collected in 1926, and 262 – collected in 1968, Table 1) were selected for analyses of stable oxygen and carbon isotope ratios ($\delta^{18}O$ and $\delta^{13}C$) and trace element ratios (Mg/Ca, Sr/Ca, Ba/Ca, Mn/Ca) based on the condition and thickness of shells and to maximize temporal coverage (Table 2). Both archived specimens remained completely intact (shell and soft tissue) during storage at LMR-ZIN and were preserved in 95% ethanol at room temperature since collection. Ethanol has not been demonstrated to affect shell geochemistry (Xia et al., 1997;Ito, 2001). The shells were rinsed with deionized (DI) water after removal from preservative and air dried prior to sectioning.

One valve from each specimen was thinly coated in polyvinyl alcohol and embedded in epoxy (Buehler Ltd., Illinois, USA). Thin sections (2 mm thick) of the shells were cut along the line of maximum growth with a low-speed diamond saw, fixed to petrographic slides with epoxy, rinsed with deionized water, and air-dried. Each thin section was polished on the sample face using 240, 320, 400, 600 grit abrasive carbide discs and a polishing cloth with 0.3 μm Al_2O_3 polishing powder according to Ambrose et al. (2006).

2.3.2. Stable Oxygen and Carbon Isotope Analysis—Shell material for oxygen and carbon stable isotope analyses was milled from thin sections with a rounded 150 μm diameter drill bit on a computer programmed Merchantek Micromill™ at the Micropaleontology Mass Spectrometry Facility (Woods Hole Oceanographic Institution (WHOI), Massachusetts, USA). We milled approximately 5-6 individual sample points per growth increment across 14-16 years from each shell (Table 2). We obtained 20-180 μg of carbonate shell material from an individual sample point by drilling 6-8 adjacent target holes (150 μm diameter, 450 μm deep) parallel to the plane of shell growth (Fig. 3). Micro-milling was targeted within the prismatic middle shell layer and within the darker, denser annual growth lines. Material from the nacreous and the organic-rich periostracum, which may be metabolically reworked or susceptible to diagenesis, was avoided. Khim et al. (2003) confirmed, using X-ray diffraction analysis, that prismatic material sampled from *S. groenlandicus* is entirely composed of aragonite.

Powdered carbonate shell samples were analyzed for oxygen and carbon stable isotopes with a ThermoFinnigan Kiel III device coupled to a Finnigan MAT252 isotope ratio mass spectrometer (IRMS) at the Micropaleontology Mass Spectrometry Facility (WHOI). Samples were reacted with 100% phosphoric acid at 70°C to liberate CO_2 inline to the IRMS. The $CaCO_3$-CO_2 fractionation factors of Friedman and O'Neal (1977) were used to calculate the isotopic composition of the carbonate samples. The samples were calibrated against the NBS-19, B1, and AtlantisII standards and all data are reported as permil (‰) VPDB in the conventional δ-notation according to the following definition:

$$\delta X(‰) = \left[\left(\frac{R_{\text{Sample}}}{R_{\text{Standard}}} \right) - 1 \right] * 1000$$

where *X* is ^{18}O or ^{13}C and R is the ratio of $^{18}O/^{16}O$ or $^{13}C/^{12}C$. Long-term precision estimates of the mass spectrometer based on analyses of NBS-19 are $\delta^{18}O$: ± 0.07 and $\delta^{13}C$: ± 0.03 (Ostermann and Curry, 2000).

Shell thin sections used for oxygen and carbon stable isotope sampling were post-processed with a Nikon SMZ1500 stereo-microscope and a 2 mega-pixel color camera at the Bates College Imaging and Computing Center (Maine USA) to calibrate individual sampling points to shell length. A composite image of each specimen was created by stitching together 20-30 images (56.4 cm × 42.3 cm) using Adobe Photoshop CS3 (Adobe Systems, San Diego, CA).

2.3.3. Trace Element Ratio Analysis—Trace element (Mg, Sr, Ba, Mn, and Ca, the latter used to normalize the other elements) analyses were conducted on shell thin-sections via a New Wave Research UP213 laser ablation system coupled to a ThermoFinnigan Element2 single-collector sector field ICP-MS. Thin-sections were prepared identically to those used for stable oxygen and carbon isotope sampling. Thin-sections were cleaned in a class 100 clean room at the Plasma Mass Spectrometry Facility (WHOI) by scrubbing with a nylon brush, rinsing with 2% HNO_3, sonicating for 5 minutes in ultra-pure H_2O, rinsing with ultra-pure H_2O, and drying for 24 hours in a laminar flow clean bench according to Ambrose et al. (2006). Approximately 12-15 laser spots (dwell time 60 sec at 10 Hz, spot size 55 μm, laser output 100% power) were shot per growth year (every 125-520 μm along the shell axis) with the last spot of a year landing on the annual growth line. This sampling scheme achieved sub-monthly to monthly resolution. Certified aragonite reference materials of known trace element composition were run every sixth spot to control for machine drift (Yoshinaga et al., 2000; Sturgeon et al., 2005). Instrument set-up was similar to that of Gunther and Heinrich (1999) as modified by Thorrold et al. (2001). External precisions (relative standard deviations) for the lab standard were as follows: Mg/Ca = 1 %, Sr/Ca = 0.6 %, Ba/Ca = 0.8 %, and Mn/Ca = 0.8 %.

The location and temporal signature integration for the stable isotope data and the trace element data were probably not synchronous. The oxygen and carbon isotope data were collected via micromilling multiple tightly grouped spots (Fig. 3), which integrated all of the growth line material, and perhaps some material secreted just prior to the growth line. The trace element data, however, were collected via high precision laser ablation, which resulted in much finer spatial (and temporal) resolution.

2.4. Environmental Data

Various environmental data sets were referenced for correlation with growth data and geochemical information obtained from *S. groenlandicus*. We examined relationships between cockle growth and the North Atlantic Oscillation Index (NAO). Data for the NAO, using the sea level pressure difference between Gibraltar and Southwest Iceland (Jones et al., 1997; Osborn et al., 1999), were obtained from (http://www.cru.uea.ac.uk/cru/data/nao.htm). We used NAO index data from the winter months (December, January, February, and March), as the signal tends to be stronger in winter, and these months precede the active period of growth.

Regional terrestrial freshwater input into the White Sea was estimated based on stream flow data from the Severnaya Dvina and Mezen' Rivers. Data from the Severnaya Dvina spans 1882-1999, and the Mezen' spans 1921-1999. While other rivers also discharge into the northern White Sea, they are much smaller than the Severnaya Dvina or Mezen' and have data records insufficiently short or sporadic for use in the present study. River discharge data were collected by Roshydromet (Russia) and accessed through R-ArcticNET (v.3.0) (http://www.r-arcticnet.sr.unh.edu/v3.0/index.html). As stream flow is highly seasonal in this region, with a very large proportion of total discharge occurring in a short period in summer, we used flows ($m^3\ s^{-1}$) during the peak month of May, and flows summed for the summer season (May, June, July).

Monthly average water temperatures and salinities were estimated at the sampling sites from a dataset presenting integrated averages from 1898 - 1993 (Matishov et al., 1998). At 50 m

water depth, long-term seasonal differences in temperature are between 4 and 6 °C, and seasonal salinity values vary by less than 0.5 PSU.

2.5. Data Treatment and Statistical Analyses

Absolute growth rates (ω parameter derived from the modeled von Bertalanffy growth function) were compared among populations using one-way analysis of variance (ANOVA) following *a priori* diagnostic tests for homogeneity of variance between groups and normal distribution of data. Standard linear regressions were used to assess relationships between SGI, NAO, and river discharge patterns. Student's t-tests were used to determine whether statistically significant differences exist between the ranges of intra- and inter-annual geochemical data. We used Pearson correlations and linear regressions to compare trace elemental ratios and stable isotope profiles within individual shells. Errors are reported as standard deviations unless otherwise stated. Statistical computations were carried out with Microsoft Excel and Statistica (ver. 6).

3. Results

3.1. Sample Population Characteristics

We analyzed 15 individual *S. groenlandicus*, collected from 8 different locations and three different time periods: 1899, 1926/1927, and 1968 in the southern Barents Sea near the entrance to the White Sea (Table 1, Fig. 1). The largest individual in our dataset was 67.1 mm, with a corresponding age of 16 years, and the average size at age 15 was 54.50 ± 9.64 mm for the 1899 collected samples, 47.09 ± 6.26 mm for the 1926/27 collected individuals, and 53.53 ±7.76 mm for the 1968 collected individuals. The age range of 15 samples was 6-22 years old, yielding time series lengths of 17 years for the cockles collected in 1899, 23 years for the cockles collected in 1926/27 and 22 years for the cockles collected in 1968. In aggregate, the samples provide a total time series of 62 years over the period 1882-1968.

Absolute growth rates (ω) varied between a maximum of 4.83 ± 1.62 in 1968 and a minimum of 3.69 ± 0.52, with an intermediate value of 4.53 ± 0.91 in 1899. These variations in the ω growth parameter were not significantly different (One-way ANOVA: $df_{3,14}$, $F = 1.45$, $P > 0.05$) between the time periods.

3.2. Standardized Growth Index (SGI)

The von Bertalanffy model was an excellent descriptor of cockle growth ($R^2 = 0.993$, $P<0.0001$). This allowed us to confidently correct for ontogenetic changes in growth with age and thereby compare actual versus the expected growth for each calendar year (SGI).

SGI varied considerably over the 17-23 year periods covered by the three time periods (Fig. 4), ranging for individual clams from a low of 0.17, 0.24, and 0.24 in the poorest growth years (1898, 1926, and 1967, respectively) to highs of 2.42, 2.74, and 2.11 in the best growth years (1887, 1918, and 1955, respectively). The mean population SGIs from each time period ranged from lows of 0.79 (1884), 0.50 (1905), and 0.46 (1966) to highs of 1.87 (1891), 1.44 (1918), and 1.65 (1955) (Fig. 4). SGI varied both within and among time periods with the highest average value (1.18 ± 0.27) in the 1899 collection and the lowest (0.94 ± 0.25) in the in 1926/27 collection. The 1899 collection had 80% of growth years with SGI over 1.0, compared to 33% for the 1926/27 collection. The SGI pattern in each time period oscillates between higher and lower values over a period of 4-6 years, rather than varying dramatically between single consecutive years (Fig. 4). This serial autocorrelation among years indicates a multi-year periodicity in the growth rates of these bivalves.

3.3. Stable Isotope and Trace Elemental Ratios

3.3.1. Stable Oxygen and Carbon Isotopes—The stable oxygen and carbon isotope profiles of both samples were characterized by seasonal cycles corresponding to the annual growth lines. $\delta^{18}O$ values were fairly uniform for most of the growing season, except for a characteristic strong depletion in ^{18}O at or just before the annual growth line (Fig. 5). The overall mean $\delta^{18}O$ value from shell 156, covering the period 1907-1922, (3.43 ± 0.59 ‰), was significantly lower than shell 262 covering the period 1946-1959, (3.73 ± 0.27 ‰) (Student's t-test, $P < 0.001$). The average $\delta^{18}O$ minima recorded on the growth lines of both shells were significantly more depleted than the average intra-annual $\delta^{18}O$ values (Student's t-tests, $P < 0.001$): 2.99 ± 0.46 ‰ vs. 3.55 ± 0.57 ‰ for 156 and 3.46 ± 0.29 ‰ vs. 3.83 ± 0.17 ‰ for 262. In shell 156, there was a large minimum in $\delta^{18}O$ in 1914, representing an approximate 3.9 ‰ deviation from the cyclic $\delta^{18}O$ pattern.

The carbon stable isotope profiles for both shells covary with the $\delta^{18}O$ profiles (Fig. 5). Similar to the $\delta^{18}O$ profiles, there are significant intra-annual differences in $\delta^{13}C$ values from annual lines and the summer material for shells 156 (Student's t-test, $P = 0.003$) and 262 (Student's t-test, $P < 0.0001$). $\delta^{13}C$ showed characteristic strong depletions in ^{13}C at or just before the annual growth line.

3.3.2. Trace Element Ratios—Trace element ratios in shell 156 reflect years 1907-1912 (Fig. 6) and in shell 262 reflects years 1957-1962 (Fig. 7). Both shells exhibit annual periodicity for all trace element ratios, corresponding to the annual growth lines on shell cross-sections. Shell 156 showed a consistent seasonal pattern in Sr/Ca and Mg/Ca ratios, where annual minima corresponded to the growth lines, followed by sharp increases in Sr/Ca, and to a lesser extent Mg/Ca, immediately following the growth line, and ending with a gradual decline approaching the next growth line (Fig. 6). This trend was closely mimicked by the Ba/Ca ratios (Sr/Ca: $R^2 = 0.49$, $P < 0.0001$; Mg/Ca: $R^2 = 0.42$, $P < 0.01$) and to a lesser degree by the Mn/Ca ratios (Sr/Ca; $R^2 = 0.16$, $P > 0.05$; Mg/Ca: $R^2 = 0.42$, $P < 0.01$).

The trace element profiles for shell 262 exhibit a similar annual cyclicity as shell 156 (Fig. 7). Annual minima for Sr/Ca are coincident with growth lines in years 1959, 1961, and 1962, however in the other years (and for all years in the Mg/Ca profile) the annual minima appears just before the growth line. In addition, there appears to be a decoupling of Sr/Ca and Mg/Ca ratios for some years that was not seen in shell 156. Ba/Ca and Mn/Ca ratios, however, showed consistent seasonal patterns, with annual minima on the growth lines and maxima in the intra-growth line material. The Ba/Ca and Mn/Ca profiles in shell 262 strongly covary ($R^2 = 0.88$, $P < 0.0001$). The patterns of Ba/Ca and Mn/Ca ratios in shell 262 were similar to those in shell 156. Shell 262 had a significantly lower average Ba/Ca ratio compared shell 156 (Student's t-test, $P = 0.006$).

3.4. Environmental Relationships

There is an inverse relationship between cockle SGI and NAO that was evident in the combined data from all three time periods (pooled $R^2 = 0.20$, $P < 0.001$), with episodes of positive NAO generally associated with low SGI and vice versa. However, this relationship is inconsistent among time periods (Fig. 8); it is strongest from 1882-1899 ($R^2 = 0.61$, $P < 0.001$), relatively weaker from 1904-1927 ($R^2 = 0.35$, $P < 0.01$), and statically insignificant from 1946-1968 ($R^2 = 0.15$, $P = 0.07$). The 1899-collected population had the highest overall SGIs, had relatively higher SGI values for a corresponding NAO, and also exhibited the strongest effect of NAO on SGI, indicated by the steeper slope of the relationship. This period was also one in which NAO values consistently negative (i.e. never exceed 1.0); the other time periods all experienced NAO values up to 2.0.

One main manifestation of the NAO is precipitation in Northern European areas, which can be reflected in river discharges (e.g. Peterson et al., 2002). In the Arctic, river discharges are strongly seasonal, with the vast majority of flow occurring in the spring and early summer. The Severnaya Dvina is the largest river to discharge into the White Sea, and has a catchment watershed of 348,000 km^2 and an average volume of 105 km^3 yr^{-1} (Peterson et al., 2002). Despite strong interannual variability, summer discharges tended to exhibit multi-annual trends at decadal-scale frequencies (Fig. 9). Discharges generally increased during the life spans of the 1899-collected individuals, were steady or decreased during the life spans of the 1926/27 collected individuals, and were quite variable during the life spans of the 1968 collected individuals (Fig. 9). There is a positive relationship ($R^2 = 0.45$) between summer river discharge and SGI (Fig. 10) in the 1899-collected population, with higher SGIs occurring during years of higher summer discharges of the Severnaya Dvina. This relationship is undetectable in the other time periods ($R^2 < 0.11$, $P > 0.05$), reflecting the reduced influence of river discharge on SGI at lower discharges.

There also appears to be an effect of river discharge on the Ba/Ca ratio in sample shell 156 with years of higher discharges of the Severnaya Dvina resulting in higher Ba/Ca ratios in the shells (Fig. 11). Summer river discharges explained 62% of the variation in the Ba/Ca isotope ratios. A similar relationship was found between Ba/Ca ratios in shell 156 and the discharge of the Mezen' River (a smaller river that also empties into the White Sea). The relationship between river discharge and Ba/Ca ratios in sample shell 262, however, was substantially weaker ($R^2 = 0.29$).

4. Discussion

Both growth rates and geochemical proxy data of the *S. groenlandicus* shells spanning from 1882-1968 from the southern Barents Sea exhibited distinct cyclic patterns on different time scales ranging from seasons to decades, reflecting scales of variability in the various components of the physical environment. Growth rates (SGI) exhibited an interannual pattern of variability consistent with large-scale climate regulation through the NAO, as locally modified through interannual variations in river discharge. $\delta^{18}O$ and $\delta^{13}C$ showed characteristic seasonal patterns, the former reflecting variations in local and regional temperature while the latter was linked to hydrographic conditions. Elemental paleothermometers support previous findings that annual growth lines in *S. groenlandicus* are deposited in winter (Ambrose et al., 2006). Meanwhile, Ba/Ca patterns provide a link to the regional influence of river discharge to the coastal hydrography of the southern Barents Sea.

4.1. Growth Rates and Environmental Relationships

Overall growth rates among the different times periods were not significantly different despite the fact that they were collected at different times, at different locations within the area (Fig. 1), and at various depths (Table 1). The 1899 collection, in particular, had some samples collected at a much greater depth (190 m) than the other populations (60-70 m). This deeper site was, however, very near the coast and the depth evidently didn't strongly influence the overall growth rates. Thus we presume some intra-regional consistency in the factors affecting growth in these populations.

The SGI pattern of relative growth among years exhibited a similar qualitative pattern in each time period, oscillating between higher and lower values over periods of 4-6 years. This serial autocorrelation among years indicates a multi-year periodicity in the growth rates of these bivalves, suggesting a response to an external driver with a similar periodicity. SGI oscillations of this temporal periodicity have been demonstrated for *S. groenlandicus* from northern Svalbard (Ambrose et al., 2006) and another cockle, *Clinocardium ciliatum*, in the northwest Barents Sea (Carroll et al., submitted). Both studies identified relationships with atmospheric

large-scale drivers, primarily with the Arctic Climate Regime Index (ACRI), but also with the NAO in Atlantic dominated areas of the Barents Sea. In the present study, we have established an inverse relationship between SGI and the NAO (Fig. 8), which was clearly apparent around the turn of the 20th century, but not detectable in the 1920's or 1960's.

The NAO is a well-known driver of atmospheric patterns in the North Atlantic region (Jones et al., 1997; Osborn et al., 1999) that is thought to broadly influence a number of climatic and meteorological patterns from the northeast coast of North America through Europe and the Mediterranean region. There is widespread evidence of the influence of the NAO on ecological components in both the terrestrial and marine ecosystems in the North Atlantic region (Ottersen et al., 2001), including phytoplankton, zooplankton, fish, and birds (Reid et al., 1998; Beaugrand et al., 2002; Durant et al., 2004; Richardson and Schoeman, 2004; Hátún et al., 2005; Heath, 2005; Perry et al., 2005; Hansen and Samuelsen, submitted). The bivalve, *Arctica islandica*, from North and Norwegian seas has been found to respond to the NAO (Schöne et al., 2005), and marine benthic species diversity and abundance patterns in Kongsfjorden (western Svalbard) exhibited strong shifts coincident with phase shifts in the NAO (Beuchel et al., 2006).

The relationship between cockles' SGI and NAO in the southern Barents Sea is apparently manifested locally through variations in discharges of the major rivers emptying into the White Sea: the Severnaya Dvina and, to a lesser extent the Mezen'. Flows of these rivers are strongly seasonal, with the vast majority of discharges occurring during a small window from May to July (Lammers et al., 2001; Ye et al., 2004). There is also strong interannual variation in river flows (Fig. 9) that is inversely related to the NAO ($R^2 = 0.42$). Further, both SGI (Fig. 10) and the Ba/Ca ratio (Fig. 11, discussed further below) are related to variations in river discharges. Large volumes of freshwater discharged episodically from rivers into the coastal oceans in the Arctic can affect myriad properties of seawater (Peterson et al., 2002; Ye et al., 2004; Milliman and Syvitski, 2002) and serve as a conduit for environmental contaminants to coastal oceans (AMAP, 1998; MacDonald et al., 2000; J. Carroll et al., 2008). Large seasonal river plumes in the Arctic can detrimentally affect marine primary producers in their immediate vicinity and reduce the diversity and biomass of benthic communities through light attenuation, osmotic stress, and smothering (e.g. Dahle et al., 1998, Denisenko et al., 2003). Beyond the plume, however, rivers can stimulate primary and secondary production by delivering large loads of organic carbon and nutrients as food sources for coastal marine communities and stabilizing the water column leading to spring blooms (Opsahl et al., 1999; Dittmar and Kattner, 2003; Stein et al., 2003). Although we have no specific information from the sites on interannual variations in primary production, the relationship between SGI and river discharge suggests that, at least in periods of high flows, the rivers are mediating the SGI patterns in the coastal sea.

It is somewhat curious that the greatest river discharges from the Severnaya Dvina occurred during the periods of NAO in the negative phase, because it is generally acknowledged that a positive NAO will drive a storm track leading to greater precipitation in the northern parts of Europe, with relatively drier conditions over the Mediterranean Region. There are, however, strong intra-regional differences in the strength of the NAO in northern Europe. For example, Uvo (2003) demonstrated that the NAO negative storm track leads to a disproportionately heavy precipitation in the coastal regions and mountains of western Norway but far less precipitation in the leeward locations in northern Scandinavia. We postulate that this intra-regional variation leads to greater river discharges, and associated higher SGIs (Fig. 10) during the negative phase of the NAO in our study region.

4.2. Stable Isotopes

We found cyclical patterns in shell $\delta^{18}O$ and $\delta^{13}C$ profiles centered around external growth lines (Fig. 5), which supports findings from previous research with a number of bivalve species (Khim et al., 2003;Simstich et al., 2005;Ambrose et al., 2006). $\delta^{18}O$ values fluctuated seasonally with patterns that were generally consistent among years for both shell 156 and 262 (Fig. 5), and were typically most depleted in ^{18}O at or just before the annual growth line. Such patterns in *S. groenlandicus* have been measured elsewhere, and are attributed to rapid cessation of growth immediately after maximum temperatures are reached (Khim et al., 2003).

The depletion in $\delta^{18}O$ values at or just before the winter growth line likely results from the combined influenced of higher water temperatures at this time of year. Using the temperature fractionation model of -0.23 ‰ $°C^{-1}$ (Grossman and Ku, 1986), and an average seasonal difference in $\delta^{18}O$ values of 0.63 ‰ in shell 156 and 0.37 ‰ in shell 262, the temperature proxy-calculated seasonal temperature change is 2.8-1.6 °C, and accounts for a substantial portion of the magnitude of the measured ~5°C seasonal range at the sampling sites (Matishov et al., 1998). Seasonal changes in water salinity occur after the spring melt and may also influence the $\delta^{18}O$ pattern. Although seasonal variations in salinity in these locations are less than 0.5 PSU at 50 m depth (Matishov et al., 1998), small change can have substantial influences in $\delta^{18}O$. With measured $\delta^{18}O$ values of freshwater in the White Sea of -15.5 ‰ (Nikolayev and Nikolayev 1988) and an estimated full ocean salinity endpoint of 0 ‰, a linear regression estimates a change of 0.44 ‰ PSU^{-1}. The resulting 0.22 ‰ range over the measured change of 0.5 PSU at the study sites can thus account for 35-59 % of the average seasonal range in $\delta^{18}O$ in addition to the temperature effect.

It is important to note that bivalve shells cannot provide a full record of the annual temperature range because the shells only record ambient environmental conditions during active growth. Thus the oxygen isotope- and mineral-derived temperature records from shell carbonate in organisms that experience dormancy are by definition truncated during dormancy (Schöne 2008).

Ecological dormancy in the Arctic winter is thought to result from a combination of extremely low temperatures and lack of food supply (e.g. Falk-Petersen et al., 2000; but see Buick and Ivany, 2004). In fact, food supply and temperature do not vary synchronously. The spring bloom results in an ample food supply to consumers in the Arctic spring when temperatures are at their lowest, and conversely, late fall in the Arctic (i.e. September-October), is a period of high water temperature yet little food availability. Seasonal patterns of food availability, as opposed to temperature, can be the primary driver of bivalve growth (Nakaoka, 1992; Nakaoka and Matsui, 1994). Evidence from the Barents region suggests that *S. groenlandicus* and *C. ciliatum* in the ice covered waters of the northwest Barents Sea and western Svalbard cease growth in late fall due to limited food availability despite warm water temperatures, and then resume growth immediately after fresh food reaches the bottom, despite water temperatures being at their coldest (Carroll et al., submitted). We suggest that the oxygen stable isotope data from the annual growth lines reflect this period of warm ambient water temperatures and food limitation as the as the cockle prepares for dormancy.

Shell 156 showed larger intra-annual variations in $\delta^{18}O$, was significantly lighter on average (by 0.3 ‰), and exhibited higher average Ba/Ca values compared to shell 262. These geochemical differences between shells may reflect differences in their relative proximity to the sources of river discharge. Shell 156 was located 150 km closer to the two main freshwater sources to the White Sea, and may reflect a more ^{18}O depleted signal overall and greater seasonality associated with increased seasonal freshwater input from the Severnaya and Mezen'

Rivers as compared to shell 262. Such spatial variability thus makes it difficult to attribute differences in $\delta^{18}O$ values between the shells to either temperature or salinity differences alone.

$\delta^{13}C$ covaries with $\delta^{18}O$ on seasonal time scales and reflects contributions of metabolic carbon as well as ambient water DIC (McConnaughey et al., 1997; Lorrain et al., 2004; Gillikin et al., 2006b; McConnaughey and Gillikin, 2008). Shell $\delta^{13}C$ values were typically lowest at or just before the annual growth line (Fig. 5). An increase in metabolic rate coincident with the rapid increase in ambient water temperatures during the fall could increase the relative contribution of ^{13}C-depeleted respired CO2 to shell carbon resulting in a depleted bulk shell $\delta^{13}C$ value. Additionally, isotopically depleted DIC corresponding to periods of low primary productivity may be incorporated directly into the shell material just before the annual growth line. While metabolic rate and local DIC $\delta^{13}C$ values most likely play the predominant role in determining shell carbon isotope values, seasonal variability in food source and $\delta^{13}C$ (McMahon et al., 2006; Søreide et al., 2006) may also contribute to shell $\delta^{13}C$ values (Michner et al., 1994; Dettman et al., 1999). These explanations are not mutually exclusive and illustrate that more research is need to fully understand the relative importance of metabolic carbon and DIC to shell $\delta^{13}C$, as has been done for other accretionary carbonate structures such as fish otoliths (Thorrold et al., 1997; Solomon et al., 2006).

4.3. Trace Elemental Ratios

Trace element profiles show strong seasonal cycles, much like the stable isotope values, for both shells 156 and 262 (Figs. 5, 6). Sr/Ca and to a lesser extent Mg/Ca exhibited annual minima coincident with the annual growth line, supporting previous research indicating that growth lines are deposited in winter when ambient temperatures are coldest (Ambrose et al., 2006). However, the Sr/Ca and Mg/Ca ratios increased significantly in early spring, contrary to typical profiles for other bivalve species (Stecher et al., 1996;Vander Putten, 2000;Gillikin et al,. 2005;Freitas et al., 2006), suggesting abrupt changes in internal physiology and/or local environmental conditions. Calibration studies indicate that Sr/Ca may be related to growth rate for some bivalve species (Gillikin et al., 2005). The significant increase in Sr/Ca and Mg/Ca ratios between winter and spring may reflect an increase in trace element incorporation due to elevated growth rates in early spring. These abrupt profiles are not expected if the bivalve was continuously recording temperature throughout the year, suggesting internal physiology may confound records of ambient water trace element concentrations during periods of limited growth (Stecher et al., 1996;Schöne, 2008).

The annual shell Ba/Ca profiles for *S. groenlandicus* exhibit clear annual periodicity with maximum values occurring early in the growth year (Figs. 5, 6). Such patterns are consistent with both the increase in primary production associated with the spring bloom and freshwater inputs during spring. Bioavailable barium for incorporation into bivalve shells typically comes from two environmental pools: food and water (Stecher et al., 1996;Gillikin et al., 2006a). Some research suggests that barium ingestion, as barite, following diatom blooms may play a role in bivalve shell Ba/Ca ratios (Stecher et al., 1996), while others (Gillikin et al., 2006a) suggest that background Ba/Ca ratios in bivalves are a more reliable proxy for ambient water Ba/Ca ratios. Gilliken et al. (2008) acknowledge that periodic spikes in Ba/Ca are under exogenous environmental control, but can not identify a satisfactory mechanistic explanation. In our bivalves, we saw a strong relationship between May discharge of the Severnaya Dvina River and maximum annual Ba/Ca in shell 156 (Fig. 11). Whether the increase in Ba/Ca ratios in our data are due to increases in ambient water Ba concentration associated with riverine discharge or increases in barium incorporation into organic matter during spring phytoplankton blooms, it is clear that spring freshwater influx was recorded in the Ba/Ca ratios of local bivalves. A similar trend was not found in shell 262, most likely due to the fact that it was located farther from the river influence. The exact mechanism for barium incorporation into

mollusk shells is not well understood (Gilliken et al., 2008), and more research needs to be conducted on the relative importance of dietary versus ambient water Ba inputs to bivalve shell Ba/Ca ratios.

The Mn/Ca profiles show similar annual cyclicity to Ba/Ca (Figs. 5, 6). Maximum values occur following the deposition of the winter growth check suggesting that elevated Mn/Ca may coincide with blooms in primary productivity in spring. Vander Putten et al. (2000) found similar patterns from Mn/Ca shell profiles and imply that they coincide with Chlorophyll-a peaks (as many as two per year). It is also apparent that particularly Mn/Ca, but also Ba/Ca, exhibit a distinct interannual pattern of decreasing peak values over the 5 year period (1907-1912) covered by the profile (Fig. 6). This proxy evidence suggests a consistent trend of decreasing primary production (Mn proxy) and/or river discharge (Ba proxy) over this period, which is supported by the measured river discharges (Fig. 9).

4.4. Summary and Conclusions

One of the great advantages of biomonitors such as clam shells is that they provide a relatively uninterrupted record of biological (i.e., growth) and physical conditions while the animal was alive. Their utility, however, hinges upon our ability to decipher the environmental records stored in the shells in light of known ecology and physiology of the organism (Schöne et al., 2008). In our study, we combined growth and geochemical information from cockles collected live at different times in order to produce a sclerochronological record covering time periods substantially greater than the lifespan of an individual cockle.

Growth rate variations (via SGI data) indicate a periodicity consistent with an overriding influence of the NAO. The mechanism by which the NAO influence is manifested in growth is via food availability, and the geochemical evidence suggests that variations in river discharge and proximity to the rivers of the White Sea are major determinants of food availability to the benthos of this region.

The growth and geochemical evidence address different, but complimentary, temporal and spatial scales. While scleorchronology can identify growth lines at sub-annual resolution (e.g. Schöne et al., 2002; 2004), the SGI results from external growth lines provides an annually and regionally integrated view, filtering out small scale variations into an overall average of yearly and regional conditions. The geochemical results, in contrast, provide much higher resolution temporal and spatial scale information and can be specifically calibrated to local environmental conditions. But these geochemical results cannot independently indicate how such variations will translate into a better or poorer growth year. By relating results of growth and shell geochemistry to local environmental conditions, particularly river discharges, over several decades, and linking these to a plausible external driver, namely the NAO, we provide a mechanistic explanation for strong physical-biological coupling in the southern Barents Sea, particularly during periods of high river discharge. We thus demonstrate the multi-proxy approach of combining the growth and geochemical results as a powerful tool in establishing baselines of ecosystem variability for assessing potential combined impacts of climatic change and increasing commercial activities in this region.

Acknowledgments

We gratefully acknowledge past financial support from Norsk Hydro, and continuing financial support from StatoilHydro, the Norwegian Research Council, and the Howard Hughes Medical Institute through Bates College. The Laboratory of Marine Research, Zoological Institute of the Russian Academy of Sciences graciously made available extensive collections of archived material, and thereby opening a window into the fascinating history of early 20th century Arctic expeditions. J. Edgerly assisted in the laboratory at Bates College and the derivation of the SGI data, the Bates College Imaging Center provided advanced photographic and imaging facilities, and V. Savinov produced the map. We also thank S. Thorrold for making laboratory facilities available at WHOI and for valuable

discussions, and S. Birdwhistell and D. Ostermann for help with the stable isotope and trace element sampling. This manuscript has been greatly improved following comments by D. Gilliken and an anonymous reviewer. This publication was made possible, in part, by NIH Grant Number P20 RR-016463 from the INBRE Program of the National Center for Research Resources. Its contents are solely the responsibility of the authors and do not necessarily represent the official views of NIH.

References

ACIA. Impacts of a warming arctic: Arctic climate impact assessment. Cambridge University Press; Cambridge, UK: 2005.

AMAP. Assessment Reports: Arctic Pollution Issues. Arctic Monitoring and Assessment Programme. Oslo, Norway: 1998. p. 859

Ambrose WG Jr, Carroll ML, Greenacre M, Thorrold S, McMahon K. Variation in *Serripes groenlandicus* (Bivalvia) growth in a Norwegian high-Arctic fjord: Evidence for local- and large-scale climatic forcing. Global Change Biology 2006;12:1595–1607.

Andrews JT. Recent and fossil growth rates of marine bivalves, Canadian Arctic, and Late-Quaternary arctic Marine environments. Paleogeography, Paleoclimatology, Paleoecology 1972;11:157–176.

Andrews JD. Effects of tropical storm Agnes on epifaunal invertebrates in Virginia estuaries. Chesapeake Science 1973;14:223–234.

Appledoorn, RS. PhD thesis. University of Rhode Island; Kingston, Rhode Island USA: 1980. The growth and life-history strategy of the soft-shell clam, *Mya arenaria* L.

Appledoorn RS. Variation in the growth rate of *Mya arenaria* and its relationship to the environment as analyzed through principal components analysis and the ω parameter of the von Bertalanffy equation. Fisheries Bulletin of the U S 1983;81:75–84.

Beaugrand G, Reid PC, Ibañez F, Lindley JA, Edwards M. Reorganization of North Atlantic marine copepod biodiversity and climate. Science 2002;296:1692–1694. [PubMed: 12040196]

Beuchel F, Gulliksen B, Carroll ML. Long-term patterns of rocky bottom macrobenthic community structure in an Arctic fjord (Kongsfjorden, Svalbard) in relation to climate variability (1980-2003). Journal of Marine Systems 2006;63:35–48.

Beukema JJ, Knoll E, Cadée GC. Effects of temperature on the length of the annual growing season of the Tellinid bivalve *Macoma balthica* (L.) living on tidal flats in the Dutch Wadden Sea. Journal of Experimental Marine Biology and Ecology 1985;90:129–144.

Blacker RW. Benthic animals as indicators of hydrographic conditions and climatic change in Svalbard waters. Fisheries Investigations Series 1957;2:1–59.

Blacker RW. Recent changes in the benthos of the West Spitzbergen fishing grounds. International Commission for Northwest Atlantic Fisheries, Special Publication 1965;6:791–794.

Buick DV, Ivany LC. 100 years in the dark: Extreme longevity of Eocene bivalves from Antarctica. Geology 2004;32:921–924.

Carré M, Bentlab I, Bruguier O, Ordinola E, Barrett NT, Fontugne M. Calcification rate influence on trace element concentrations in aragonitic bivalve shells: Evidences and mechanisms. Geochimica et Cosmochimica Acta 2006;70:4906–4920.

Carroll J, Savinov V, Savinova T, Dahle S, McCrea R, Muir DCG. PCBs, PBDEs and pesticides released to the Arctic Ocean by the Russian Rivers Ob and Yenisei. Environmental Science and Technology 2008;42:69–74. [PubMed: 18350877]

Carroll ML, Denisenko SG, Renaud PE, Ambrose WG Jr. Benthic infauna of the seasonally ice-covered western Barents Sea: Patterns and relationships to environmental forcing. Deep Sea Research II 2008a;55:2340–2351.10.1016/j.dsr2.2008.05.022

Carroll, ML.; Denisenko, SG.; Voronkov, A.; Ambrose, WG., Jr; Henkes, GA.; Bosheim, S.; Fredheim, B.; Gulbrandsen, TR. Arctic bivalves as indicators of environmental variation. Proceedings of the SPE 9th International Conference on Health Safety and Environment; 15-17 April 2008; Nice, France. 2008b. SPE111-558

Carroll ML, Ambrose WG Jr, Levin BS, Ratner AR, Ryan SK, Henkes GA. Climatic Regulation of *Clinocardium ciliatum* (bivalvia) growth in the northwestern Barents Sea. Journal of Marine Systems. submitted

Dayton, PK. Polar benthos. In: Smith, WO., editor. Polar Oceanography, Part B Chemistry, Biology, and Geology. Academic Press; San Diego: 1990. p. 631-685.

Dahle S, Denisenko SD, Denisenko NV, Cochrane SJ. Benthic fauna in the Pechora Sea. Sarsia 1998;83:183–210.

Dekker R, Beukema J. Relations of summer and winter temperatures with dynamics and growth of two bivalves, *Tellina tenuis* and *Abra tenuis*, on the northern edge of their intertidal distribution. Journal of Sea Research 1999;42:207–220.

Denisenko, SG.; Denisenko, SV.; Dahle, S. Baseline Russian investigations of the bottom fauna in the southeastern part of the Barents Sea. In: Skjoldal, HR.; Hopkins, C.; Erikstad, KE.; Leinaas, HP., editors. Ecology of Fjords and Coastal Waters. Elsevier Science; Amsterdam: 1995. p. 293-302.

Denisenko SG, Denisenko NV, Lehtonen KK, Andersin AB, Laine AO. Macro-zoobenthos of the Pechora Sea (southeastern Barents Sea): Community structure and spatial distribution in relation to environmental conditions. Marine Ecology Progress Series 2003;258:109–123.

Dettman DL, Reische AK, Lohmann KC. Controls on the stable isotope composition of seasonal growth bands in aragonitic fresh-water bivalves (unionidae). Geochimica et Cosmochimica Acta 1999;63:1049–1057.

Dittmar T, Kattner G. The biogeochemistry of the river and shelf ecosystem of the Arctic Ocean: a review. Marine Chemistry 2003;83:103–120.

Drinkwater K. The regime shift of the 1920s and 1930s in the North Atlantic. Progress in Oceanography 2006;68:134–151.

Durant JM, Anker-Nielssen T, Hjermann DØ, Stenseth NC. Regime Shifts in the breeding of an Atlantic puffin population. Ecology Letters 2004;7:388–394.

Dutton AL, Lohmann KC, Zinsmeister WJ. Stable isotope and minor element proxies for Eocene climate of Seymour Island, Antarctica. Paleoceanography 2002;17(2)10.1029/2000PA000593

Falk-Peteren S, Hop H, Budgell WP, Hegseth EN, Korsnes R, Lovyning TB, Orbaek JB, Kawamura T, Shirasawa K. Physical and ecological processes in the marginal ice zone of the northern Barents Sea during the summer melt period. Journal of Marine Systems 2000;27:131–159.

Feder HM, Naidu AS, Jewett SW, Hameedi JM, Johnson WR, Whitledge TE. The northeastern Chukchi Sea: benthos-environmental interactions. Marine Ecology Progress Series 1994;111:171–190.

Freitas PS, Clarke LJ, Kennedy H, Richardson CA, Abrantes F. Environmental and biological controls on elemental (Mg/Ca, Sr/Ca and Mn/Ca) ratios in shells of the king scallop *Pecten maximus*. Geochimica et Cosmochimica Acta 2006;70:5119–5133.

Friedman, I.; O'Neal, JR. Compilation of stable fractionation factors of geochemical interest. In: Fleischer, M., editor. Data of Geochemistry, U S Geological Survey Professional Paper 440-KK. Vol. 6th. Reston, Virginia, USA: 1977.

Fritts, HC. Tree Rings and Climate. Academic Press; New York: 1976. p. 567

Gallucci VE, Quinn ZJ II. Reparameterizing, fitting, and testing a simple growth model. Transactions of the American Fisheries Society 1979;108:14–25.

Gillikin DP, Lorrain A, Navez J, Taylor JW, Andre L, Keppens E, Baeyens W, Dehairs F. Strong biological controls on Sr/Ca ratios in aragonitic marine bivalve shells. Geochemistry, Geophysics, Geosystems 2005;6:Q05009.10.1029/2004GC000874

Gillikin DP, Dehairs F, Lorrain A, Steenmans D, Baeyens W, Andre L. Barium uptake into the shells of the common mussel (*Mytilus edulis*) and the potential for estuarine paleo-chemistry reconstruction. Geochimica et Cosmochimica Acta 2006a;70:395–407.

Gillikin DP, Lorrain A, Bouillon S, Willenz P, Dehairs F. Shell carbon isotopic composition of Mytilus edulis shells: relation to metabolism, salinity, $\delta^{13}C_{DIC}$ and phytoplankton. Organic Geochemistry 2006b;37:1371–1382.

Gillikin DP, Lorrain A, Paulet YM, André L, Dehairs F. Synchronous barium peaks in high-resolution profiles of calcite and aragonite marine bivalve shells. Geo-Marine Letters 2008;28:351–358.10.1007/s00367-008-0111-9

Grossman EL, Ku TL. Carbon and oxygen isotopic fractionation in biogenic aragonite: Temperature effects. Chemical Geology 1986;59:59–74.

Gunther D, Heinrich CA. Enhanced sensitivity in laser ablation-ICP mass spectrometry using helium-argon mixtures as aerosol carrier. Journal of Analytical Atomic Spectrometry 1999;14:1363–1368.

Hansen C, Samuelsen A. Interannual variability of the primary production in the Norwegian Sea: relation to the NAO in a numerical model. Marine Ecology Progress Series. submitted

Hátún H, Sandø AB, Drange H, Hansen B, Valdimarsson H. Influence of the Antlatic Subpolar Gyre on the Thermohaline Circulation. Science 2005;309:1841–1844. [PubMed: 16166513]

Heath MR. Changes in the structure and function of the North Sea fish foodweb, 1973-2000, and impacts of fishing and climate. ICES Journal of Marine Science 2005;62:405–411.

Ito, E. Application of stable isotope techniques to inorganic and biogenic carbonates. In: Last, WM.; Smol, JP., editors. Tracking Environmental Change Using Lake Sediments. Springer; Netherlands: 2001. p. 351-371.

Jones DS. Annual growth increments in shells of *Spisula solidissima* recorded marine temperature variability. Science 1981;211:165–165. [PubMed: 17757267]

Jones DS, Quitmyer IR. Marking time with bivalve shells: Oxygen isotopes and season of annual increment formation. Palaios 1996;11:340–346.

Jones DS, Arthus MA, Allard DJ. Sclerochronological records of temperature and growth from shells of *Mercenaria mercenaria* from Narragansett Bay, Rhode Island. Marine Biology 1989;102:225–234.

Jones PD, Jonsson T, Wheeler D. Extension to the North Atlantic Oscillation using early instrumental pressure observations from Gibraltar and South-West Iceland. International Journal Climatology 1997;17:1433–1450.

Khim BK, Krantz DE, Brigham-Grette J. Stable isotope profiles of Last Interglacial (Pelukian Transgression) mollusks and paleoclimate implications in the Bering Strait Region. Quaternary Science Reviews 2001;20:463–483.

Khim BK. Stable isotope profiles of Serripes groenlandicus shells. I. Seasonal and interannual variations of Alaskan Coastal Water in the Bering and Chukchi Seas. Geosciences Journal 2002;6:257–267.

Khim BK, Kranz DE, Cooper LW, Grebmeier JM. Seasonal discharge to the western Chukchi Sea shelf identified in stable isotope profiles of mollusk shells. Journal of Geophysical Research 2003;108 (C9):3300.10.1029/2003JC001816

Kilada RW, Roddick D, Mombourquette K. Age determination, validation, growth and minimum size of sexual maturity of the Greenland Smoothcockle (*Serripes groenlandicus*, Bruguiere, 1789) in Eastern Canada. Journal of Shellfish Research 2007;26(2):443–450.

Klein RT, Lohmann KC, Thayer CW. Bivalve skeletons record sea-surface temperature and $\delta^{18}O$ via Mg/Ca and $^{18}O/^{16}O$ ratios. Geology 1996;24:415–418.

Lammers RB, Shiklomanov AI, Vörösmarty CJ, Fekete BM, Peterson BJ. Assessment of contemporary Arctic river runoff based on observational discharge records. Journal of Geophysical Research 2001;106(D4):3321–3334.

Lewis DE, Cerrato RM. Growth uncoupling and the relationship between shell growth and metabolism in the soft shell clam *Mya arenaria*. Marine Ecology Progress Series 1997;158:177–189.

Loeng, H. Ecological features of the Barents Sea. In: Rey, L.; Alexander, V., editors. Proceedings of the 6th International Conference Committee on the Arctic; 1989. p. 327-365.

Loeng H. Features of the physical oceanographic conditions in the Barents Sea. Polar Research 1991;10:5–18.

Loeng H, Ozhigin V, Ådlandsvik B. Water fluxes through the Barents Sea. ICES Journal of Marine Science 1997;54:310–317.10.1006/jmsc.1996.0165

Lorrain A, Paulet YM, Chauvaud L, Dunbar R, Mucciarone D, Fontugne M. $\delta^{13}C$ variation in scallop shells: increasing metabolic carbon contribution with body size? Geochimica et Cosmochimica Acta 2004;68:3509–3519.

Macdonald RW, Barrie LA, Bidleman TF, Diamond ML, Gregor DJ, Semkin RG, Strachan WMJ, Li YF, Wania F, Alaee M, Alexeeva LB, Backus SM, Bailey R, Bewers JM, Gobeil C, Halsall CJ, Harner T, Hoff JT, Jantunen LMM, Lockhart WL, Mackay D, Muir DCG, Pudykiewicz J, Reimer KJ, Smith JN, Stern GA, Schroeder WH, Wagemann R, Yunker MB. Contaminants in the Canadian Arctic: 5 years of progress in understanding sources, occurrence and pathways. Science of the Total Environment 2000;254:93–234. [PubMed: 10885446]

Matishov, G.; Zyev, A.; Golubev, V.; Slobodkin, V.; Levitus, S.; Smolyar, I. World Data Center – A for Oceanography, International Ocean Atlas Series. Vol. 1. NOAA Atlas NESDIS 26; 1998. Climatic

Atlas of the Barents Sea 1998: Temperature, salinity, oxygen. Digital Media; also online at: http://www.nodc.noaa.gov/OC5/barsea/barindex1.html

McConnaughey TA, Burdett J, Whelan JF, Paull CK. Carbon isotopes in biological carbonates: Respiration and photosynthesis. Geochimica et Cosmochimica Acta 1997;61:611–622.

McConnaughey TA, Gillikin DP. Carbon isotopes in mollusk shell carbonates. Geo-Marine Letters 2008;28:287–299.

McDonald, J.; Feder, HM.; Hoberg, M. Bivalve mollusks of the Southeastern Bering Sea. In: Hood, DW.; Calder, JA., editors. The Eastern Bering Sea Shelf: Oceanography and Resources. University of Washington Press; Seattle: 1981. p. 1155-1204.

McMahon KW, Ambrose WG Jr, Johnson BJ, Sun MY, Lopez GR, Clough LM, Carroll ML. Benthic community response to ice algae and phytoplankton in Ny Ålesund, Svalbard. Marine Ecology Progress Series 2006;310:1–14.

Michener, RH.; Shell, DM. Stable isotope ratios as tracers in marine aquatic food webs. In: Lajtha, K.; Michener, RH., editors. Stable Isotopes in Ecology and Environmental Studies. Blackwell Scientific Publications; 1994. p. 138-157.

Milliman JD, Syvitski JPM. Geomorphic/tectonic control of sediment discharge to the oceans: The importance of small mountainous rivers. Journal of Geology 1992;100:525–544.

Morison JH, Aagaard K, Falkner KK, Hatakeyama K, Moritz R, Overland JE, Perovich D, Shmada K, Steele M, Takizawa T, Woodgate R. North Pole Environmental Observatory delivers early results. Eos 2002;83:360–361.

Müller-Lupp T, Bauch HA. Linkage of Artic shelf atmospheric circulation and Siberian shelf hydrography: a proxy validation using δ18O records of bivalve shells. Global Planetary Change 2005;48:175–186.

Nakaoka M. Spatial and seasonal variation in growth rate and secondary production of *Yoldia notabilis* in Otsuchi Bay, Japan, with reference to the influence of food supply from the water column. Marine Ecology Progress Series 1992;88:215–223.

Nakaoka M, Matsui S. Annual variation in the growth rate of *Yoldia notabilis* (Bivalvia: Nuculanidae) in Otsuchi Bay northeastern Japan analyzed using shell microgrowth patterns. Marine Biology 1994;119:397–404.

Nikolayev VI, Nikolayev SD. Formation of the oxygen isotopic composition of waters of the White Sea Basin, Water Resources 1988;14:408–411.

Osborn TJ, Briffa KR, Tett SFB, Jones PD, Trigo RM. Evaluation of the North Atlantic Oscillation as simulated by a coupled climate model. Climate Dynamics 1999;15:685–702.

Opsahl S, Benner R, Amon RMW. Major flux of terrigenous dissolved organic matter through the Arctic Ocean. Limnology and Oceanography 1999;44:2017–2023.

Ostermann DR, Curry WB. Calibration of stable isotopic data: An enriched $\delta^{18}O$ standard used for source gas mixing detection and correction. Paleoceanography 2000;15:353–360.

Ottersen G, Stenseth NC. Atlantic climate variability governs oceanographic and ecological variability in the Barents Sea. Limnology and Oceanography 2001;46:1774–1780.

Ottersen G, Planque B, Belgrano A, Post E, Reid PC, Stenseth NC. Ecological effects of the North Atlantic Oscillation. Oecolgica 2001;128:1–14.

Pannella G. Fish otoliths: daily growth layers and periodical patterns. Science 1971;173:1124–1127. [PubMed: 5098955]

Perry AL, Low PJ, Ellis JR, Reynolds JD. Climate change and distribution shifts in marine fisheries. Science 2005;308:1912–1915. [PubMed: 15890845]

Peterson BJ, Holmes RM, McClelland JW, Vörösmarty CJ, Lammers RB, Shiklomanov AI, Shiklomanov IA, Rahmstorf S. Increasing river discharge to the Arctic Ocean. Science 2002;298:2171–2173. [PubMed: 12481132]

Reid PC, Planque B, Edwards M. Is observed variability in long-term results of the Continuous Plankton Recorder survey a response to climate change? Fisheries Oceanography 1998;7:282–288.

Renaud P, Morata N, Carroll ML, Denisenko SG, Reigstad M. Pelagic-benthic coupling in the western Barents Sea: processes and time-scales. Deep-Sea Research II 2008;55:2372–2380.10.1016/j.dsr2.2008.05.017

Rhoads, DC.; Lutz, RA., editors. Skeletal Growth of Aquatic Organisms: Biological Records of Environmental Change. Plenum Press; New York: 1980. p. 750

Richardson AJ, Schoeman DS. Climate impact on plankton ecosystems of the North Atlantic. Science 2004;305:1609–1612. [PubMed: 15361622]

Richardson CA. Molluscs as archives of environmental change. Oceanography and Marine Biology: An Annual Review 2001;39:103–164.

Sakshaug E. Biomass and productivity distrubutions and their variability in the Barents Sea. ICES Journal of Marine Science 1997;54:341–350.

Schöne BR, Lega J, Flessa KW, Goodwin DH, Dettman DL. Reconstructing daily temperatures from growth rates of the intertidal bivalve mollusk *Chione cortezi* (northern Gulf of California, Mexico). Palaeogeography, Palaeoclimatology, Palaeoecology 2002;184:131–146.

Schöne BR, Freyre Castro AD, Fiebig J, Houk SD, Oschmann W, Kröncke I. Sea surface water temperatures over the period 1884–1983 reconstructed from oxygen isotope ratios of a bivalve mollusk shell (*Arctica islandica*, southern North Sea). Palaeogeography, Palaeoclimatology, Palaeoecology 2004;212:215– 232.

Schöne BR, Houk SD, Freyre Castro AD, Fiebig J, Oschmann W, Kröncke I, Dreyer W, Gosselck F. Daily growth rates in shells of *Arctica islandica*: Assessing sub-seasonal environmental controls on a long-lived bivalve mollusk. Palaios 2005;20:78–92.

Schöne BR. The curse of physiology—challenges and opportunities in the interpretation of geochemical data from mollusk shells. Geo-Marine Letters 2008;28:269–285.

Simstich J, Harms I, Karcher MJ, Erlenkeuser H, Stanovoy V, Kodina L, Bauch D, Spielhagen RF. Recent freshening in the Kara Sea (Siberia) recorded by stable isotopes in Arctic bivalve shells. Journal of Geophysical Research 2005;110:C08006.10.1029/2004JC002722

Solomon CT, Weber PK, Cech JJ Jr, Ingram BL, Conrad ME, Machavaram MV, Pogodina AR, Franklin RL. Experimental determination of the sources of otolith carbon and associated isotopic fractionation. Canadian Journal of Fisheries and Aquatic Sciences 2006;63:79–89.

Stecher HA, Krantz DE, Lord CJ, Luther GW, Bock KW. Profiles of strontium and barium in *Mercenaria mercenaria* and *Spisula solidissima* shells. Geochimica et Cosmochimica Acta 1996;60:3445–3456.

Stein, R.; Fahl, K.; Fütterer, DK.; Galimov, EM.; Stepanets, OV., editors. Proceedings in Marine Science. Elsevier; 2003. Siberian river run-off in the Kara Sea: Characterisation, quantification, variability, and environmental significance; p. 496

Stenseth, NC.; Ottersen, G.; Hurrell, JW.; Belgrano, A., editors. The North Atlantic: A comparative perspective. Oxford University Press; 2004. Marine Ecosystems and Climate Variation; p. 252

Sturgeon RE, Willie SN, Yang L, Greenberg R, Spatz RO, Chen Z, Scriver C, Clancy V, Lam JW, Thorrold S. Certification of a fish otolith reference material in support of quality assurance for trace element analysis. Journal of Analytical Atomic Spectrometry 2005;20:1067–1071.

Søreide JE, Hop H, Falk-Petersen S, Hegseth EN, Carroll ML. Seasonal food web structures and sympagic-pelagic coupling in the European Arctic revealed by stable isotopes and a two-source food web model. Progress in Oceanography 2006;71:59–87.

Tallqvist MI, Sundet JH. Annual growth of the cockle *Clinocardium ciliatum* in the Norwegian Arctic (Svalbard area). Hydrobiologia 2000;440:331–338.

Thompson I, Jones DS, Dreibelbis D. Annual internal growth banding and life history of the ocean quahog *Arctica islandica* (Mollusca: Bivalvia). Marine Biology 1980;57:25–34.

Thorrold SR, Campana SE, Jones CM, Swart PK. Factors determining $\delta^{13}C$ and $\delta^{18}O$ fractionation in aragonitic otoliths of marine fish. Geochimica et Cosmochimica Acta 1997;61:2909–2919.

Thorrold SR, Latkoczy C, Swart PK, Jones CM. Natal homing in a marine fish population. Science 2001;12:297–299. [PubMed: 11209078]

Torres ME, Barry JP, Hubbard DA, Suess E. Reconstructing the history of fluid flow at cold seep sites from Ba/Ca ratios in vasicomyid clam shells. Limnology and Oceanography 2001;46:1701–1708.

Uvo CB. Analysis and regionalization of northern European winter precipitation based on its relationship with the North Atlantic Oscillation. International Journal of Climatology 2003;23:1185–1194.

Vander Putten E, Dehairs F, Keppens E, Baeyens W. High resolution distribution of trace elements in the calcite shell layer of modern *Mytilus edulis*: Environmental and biological controls. Geochimica et Cosmochimica Acta 2000;64:997–1011.

Vinje T, Knambekk AS. Barents Sea drift ice characteristics. Polar Research 1991;10:59–68.

Wassmann P, Reigstad M, Haug T, Rudels B, Carroll ML, Hop H, Gabrielsen GW, Falk-Petersen S, Denisenko SG, Arashkevich E, Slagstad D, Pavlova O. Food webs and carbon flux in the Barents Sea. Progress in Oceanography 2006;71:232–287.

Weidman CR, Jones GA, Lohmann KC. The long-lived mollusk *Arctica islandica*: A new paleoceanographic tool for the reconstruction of bottom temperatures for the continental shelves if the northern North Atlantic Ocean. Journal of Geophysical Research 1994;99:18305–18314.

Witbaard R, Duineveld GCA, de Wilde PAWJ. Geographic differences in growth rates of *Arctica islandica* (Mollsuca: Bivalvia) from the North Sea and adjacent waters. Journal of the Marine Biological Association of the UK 1999;79:907–915.

Xia J, Ito E, Engstrom DR. Geochemistry of ostracode calcite: Part 1. An experimental determination of oxygen fractionation. Geochimica et Cosmochimica Acta 1997;61:377–382.

Ye H, Ladochy S, Yang T, Zhang T, Zhang X, Ellison M. The Impact of Climatic Conditions on Seasonal River Discharges in Siberia. Journal of Hydrometeorology 2004;5:286.

Yoshinaga J, Nakama A, Morita M, Edmonds JS. Fish otolith reference material for quality assurance of chemical analysis. Marine Chemistry 2000;9:91–97.

Zenkevich, L. Biology of the Seas of the USSR. George Allen & Unwin; London: 1963.

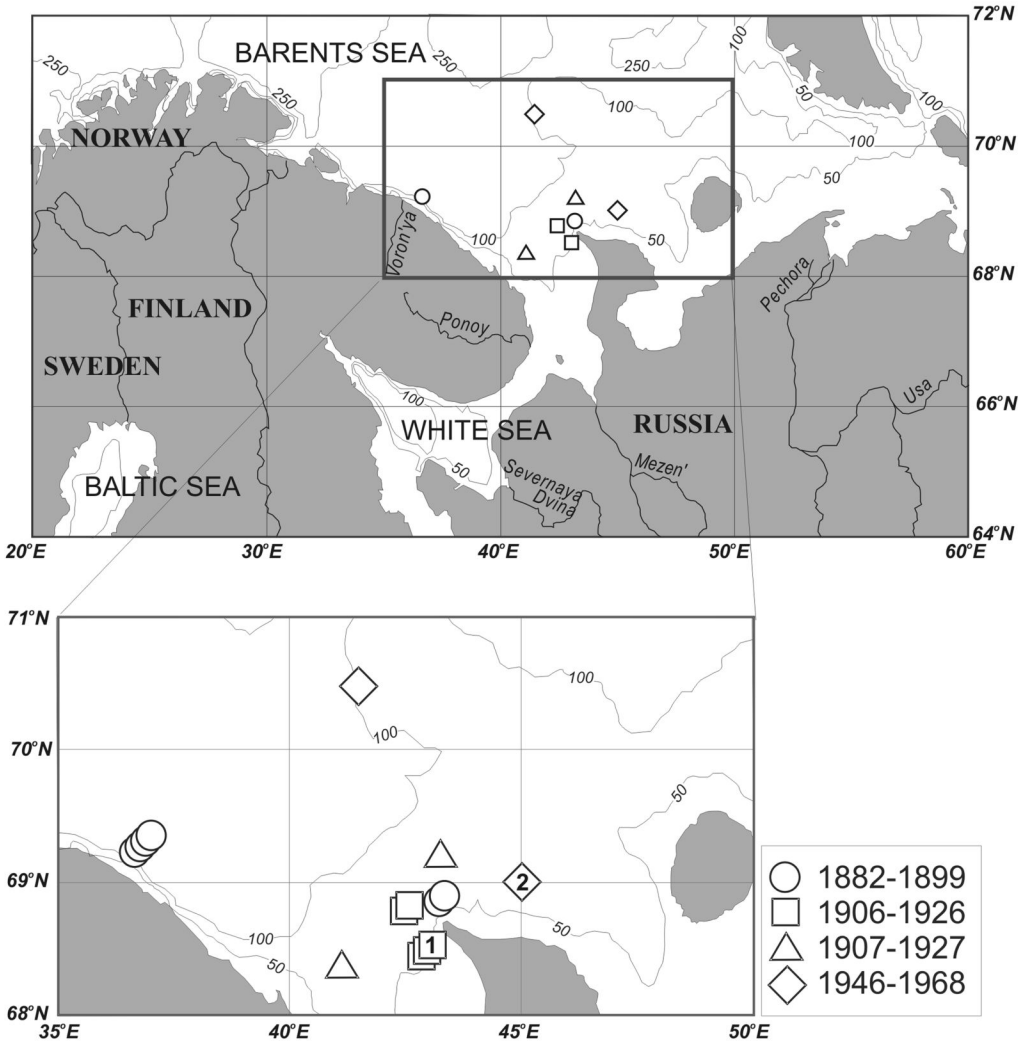

Figure 1.

Map showing the collection locations of *S. groenlandicus* analyzed for growth rates and stable isotopes/trace elements ((1) is shell 156 and (2) is shell 262), coded for time of collection. The upper map is a larger view of the inset region in the southeast Barents Sea outlined in a bold box. Major river systems, including Severnaya Dvina and Mezen', are shown in the large-scale map.

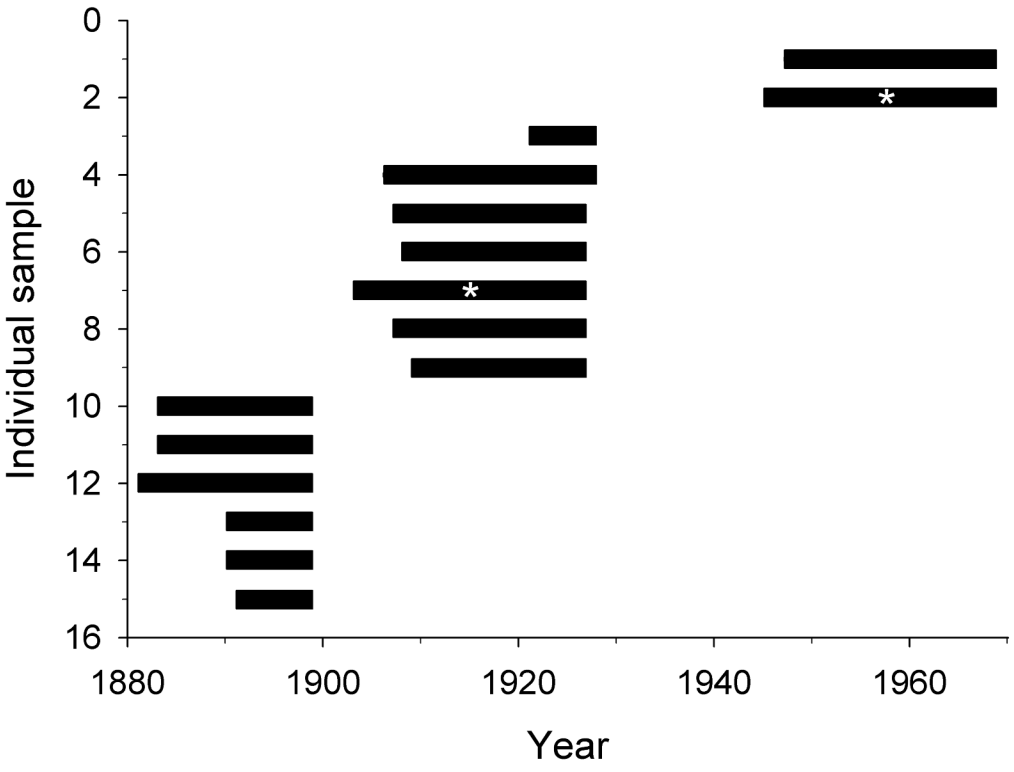

Figure 2.
Schematic showing the timeframe represented by each of the 15 individual *S. groenlandicus* analyzed for growth patterns. Lifespan was determined from the collection date of the individuals and an analysis of the annual growth increments on the shell. Asterices mark individuals sampled for stable isotope and elemental ratios.

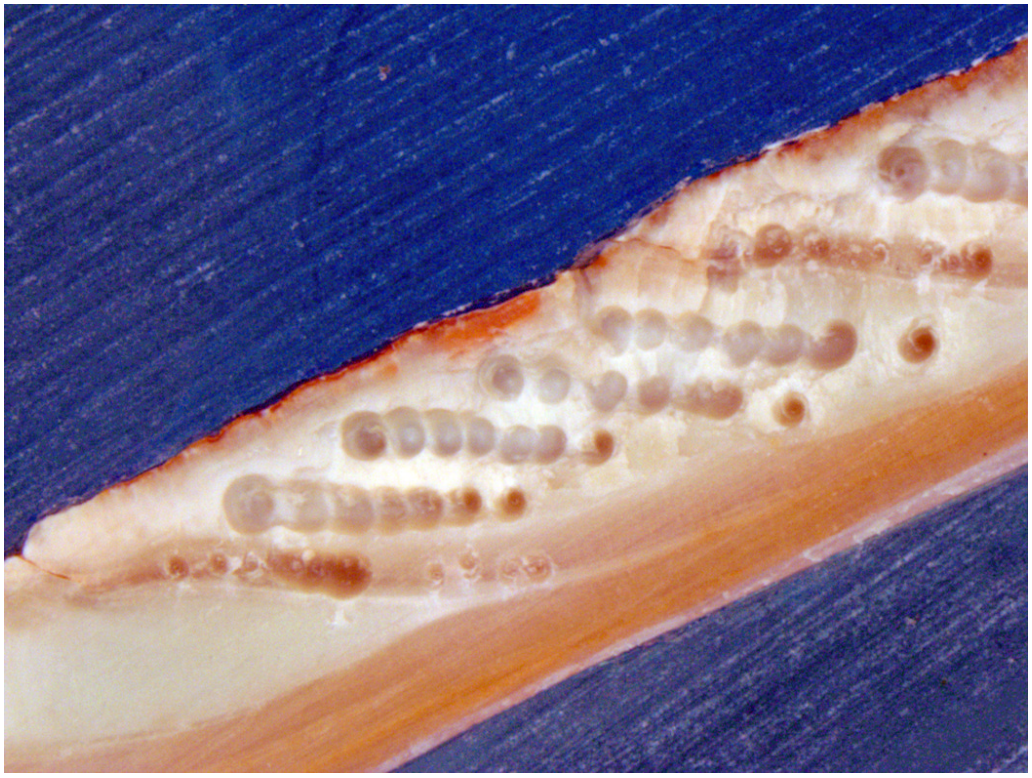

Figure 3.
Photo a portion of the cross-section of shell 156, showing the pattern of micromill drill holes. Adjacent holes were drilled along the axis of shell growth and pooled to obtain enough material for stable isotopic analysis. This photo shows 7 sets of pooled samples over 1+ years of growth and 2 growth lines.

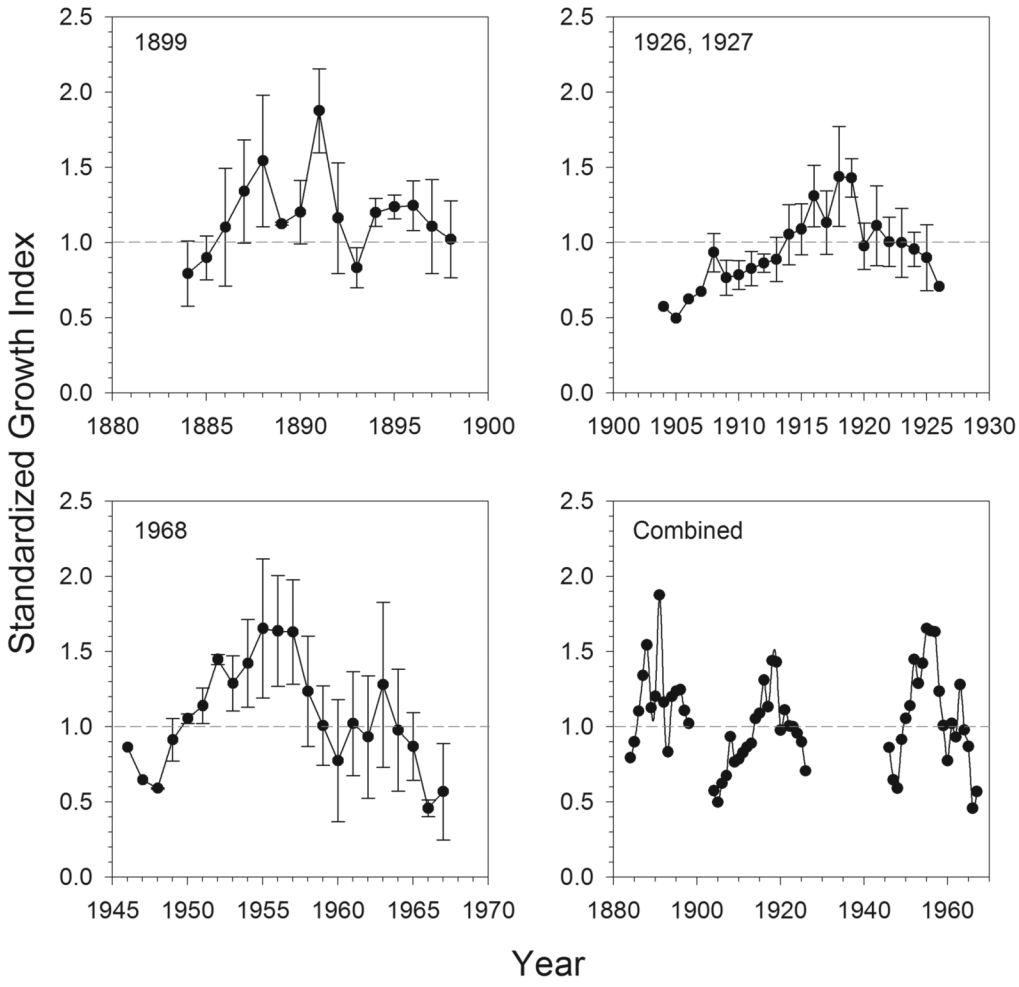

Figure 4.

Temporal SGI patterns of S. groenlandicus over the 3 collection periods (1899, 1926/1927, and 1968), and combined on a single time scale. The dashed line in each plot represents an SGI of 1.0, with values above this line indicating better than expected years of growth, and values below the line reflecting less than expected growth for those years. Error bars (±1SD) are shown when the sample size exceeded 1 individual; error bars are excluded on the combined plot to enhance readability of patterns.

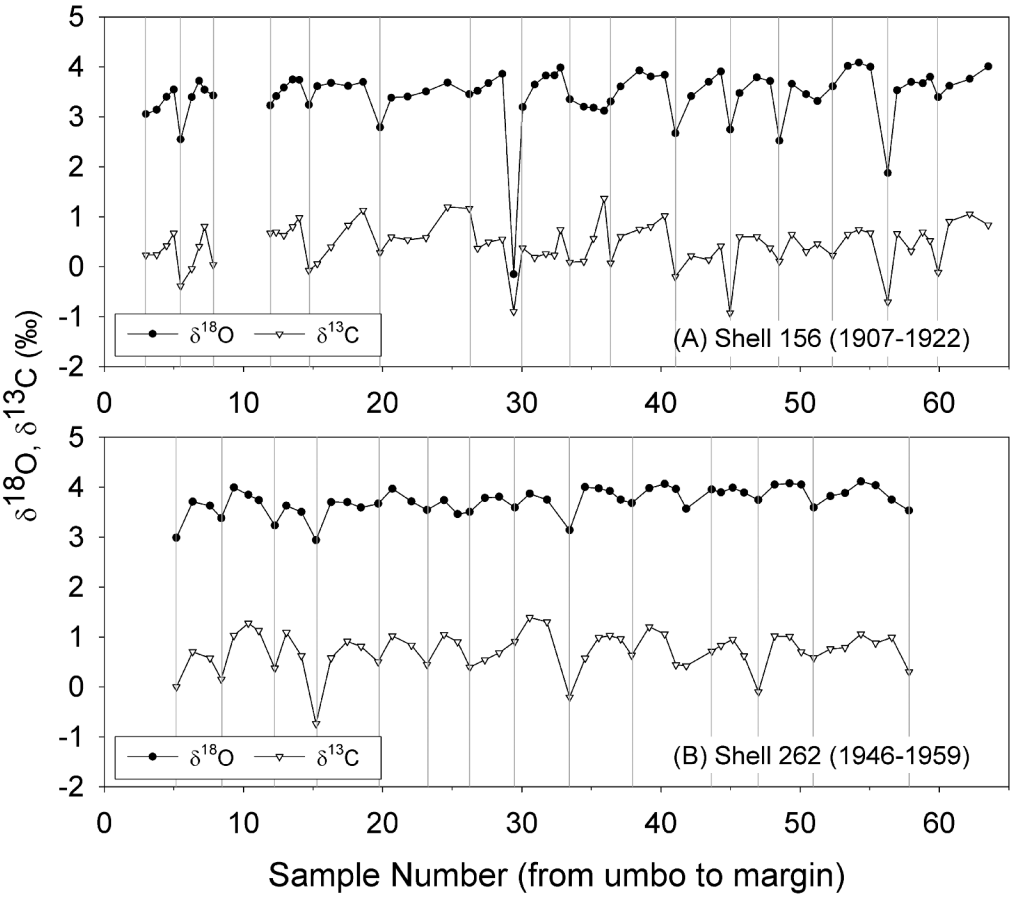

Figure 5.
Stable oxygen and carbon isotope profiles of *S. groenlandicus* specimens from (A) 1907-1922 (shell 156) and (B) 1946-1959 (shell 262). The vertical dashed lines represent the annual growth bands identified in shell cross-section. Stable isotopes are plotted with the most enriched values at the top of the y-axis.

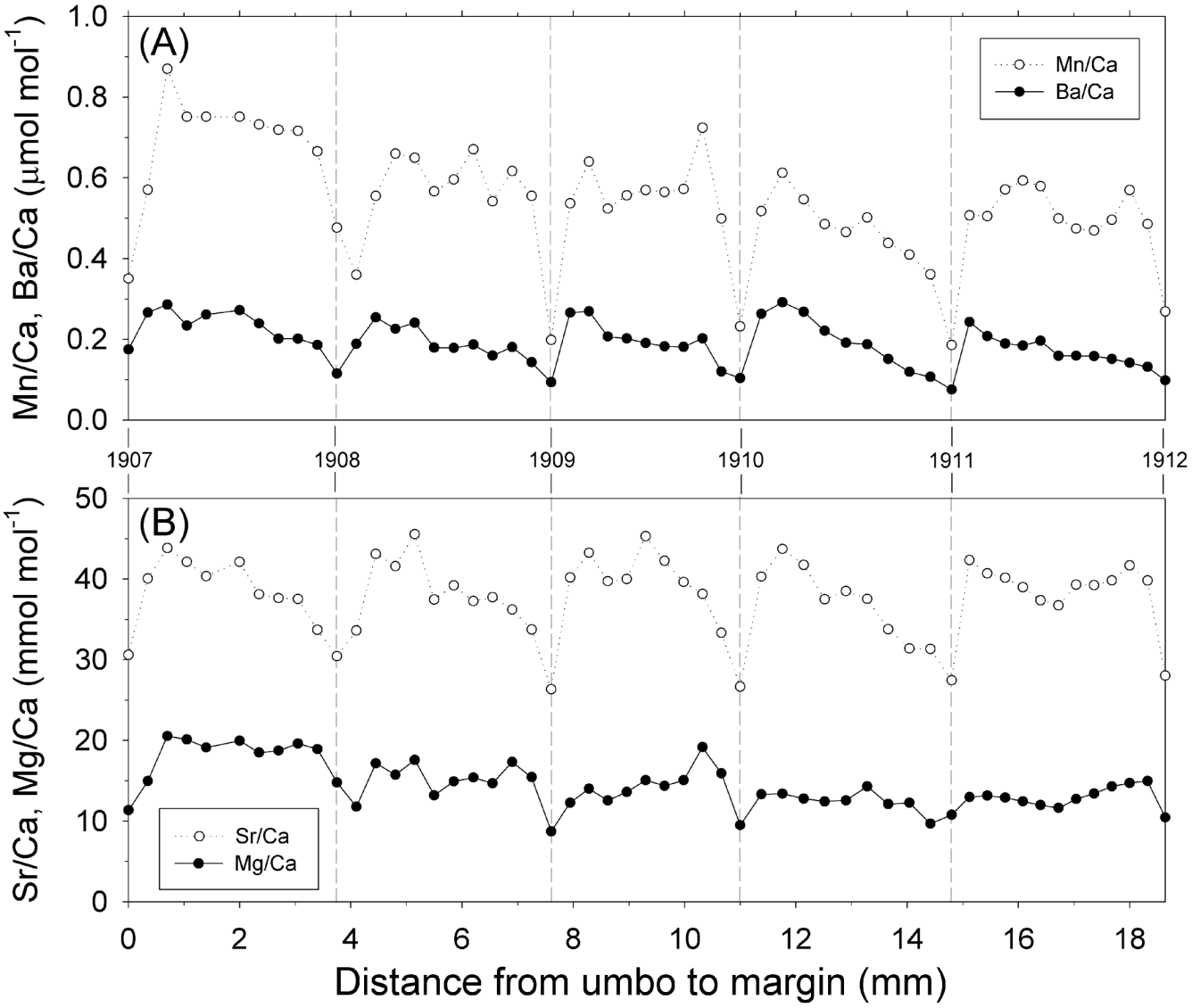

Figure 6.
Shell profiles of (A) Mn/Ca and Ba/Ca (µmol mol^{-1}) and (B) Sr/Ca and Mg/Ca ratios (mmol mol^{-1}) for the *S. groenlandicus* specimen 156, collected in July 1926. Sample distance is measured from the first growth band sampled closest to the ventral margin. The vertical dashed lines represent the annual growth bands identified in shell cross-section.

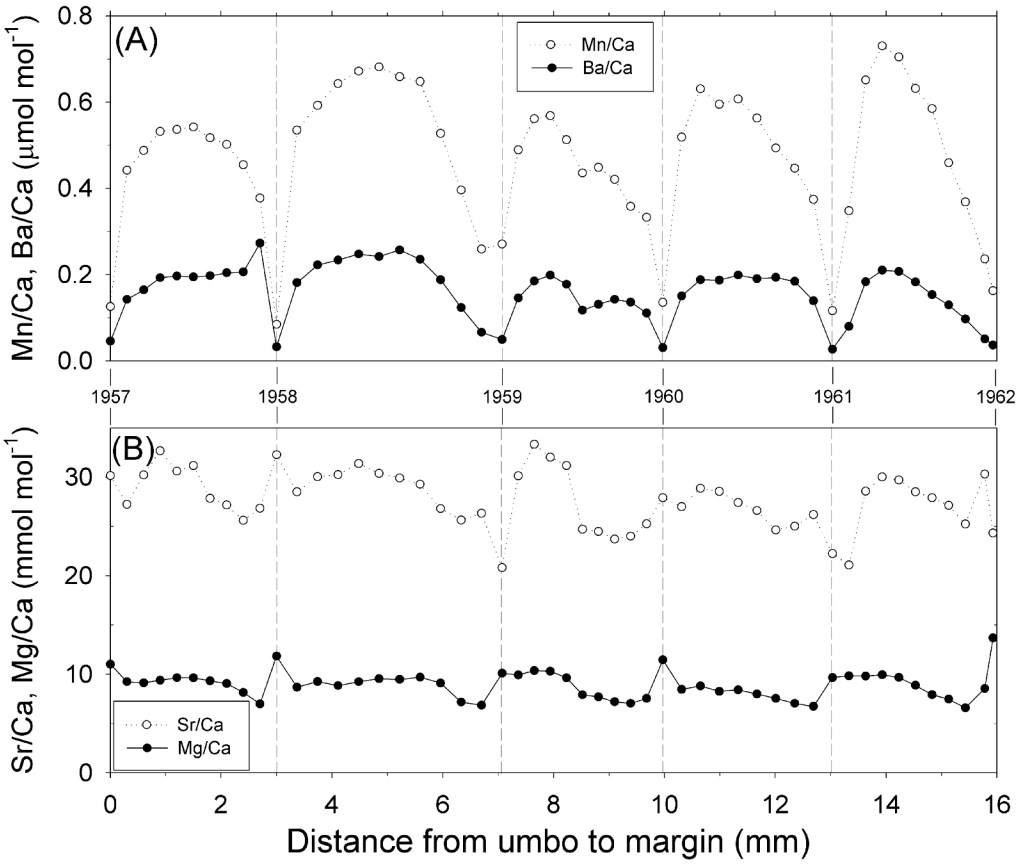

Figure 7.

Shell profiles of (A) Mn/Ca and Ba/Ca (μmol mol^{-1}) and (B) Sr/Ca and Mg/Ca ratios (mmol mol^{-1}) for the *S. groenlandicus* specimen 262, collected in July 1968. Sample distance is measured from the first growth band sampled closest to the ventral margin. The vertical dashed lines represent the annual growth bands identified in shell cross-section.

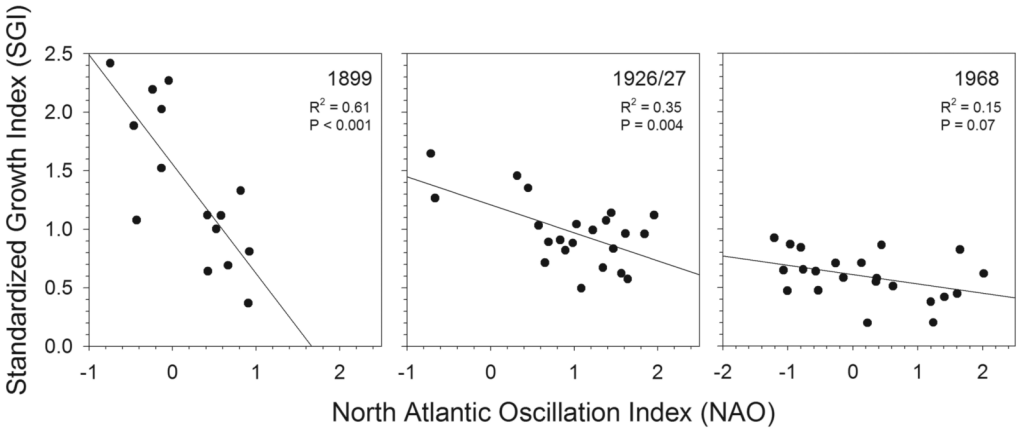

Figure 8.

Relationship between the North Atlantic Oscillation Index (NAO) and the Standardized Growth Index for *S. groenlandicus* collected in 1899, 1926/27, and 1968. NAO is calculated in the 12-month period ending in August of the growth year. Lines are least squared results from linear regressions.

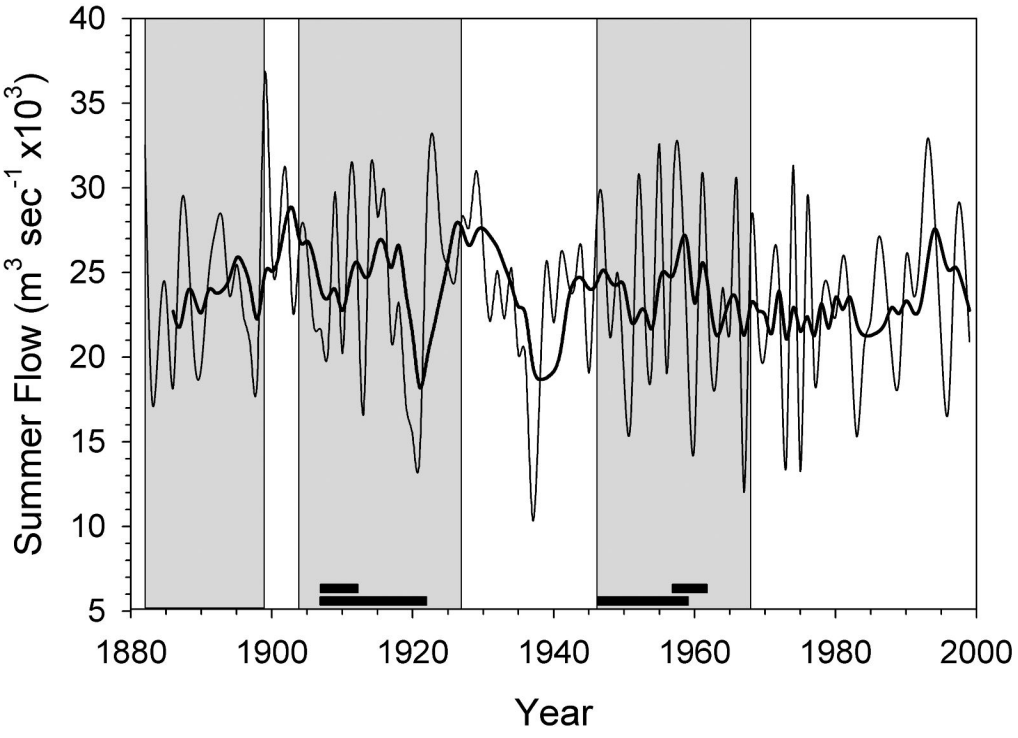

Figure 9.

Summer flow (m^3 sec^{-1} × 10^3 for the months of May, June, and July) of the Severnaya Dvina measured at the Ust'-Pinega gauge for the period 1881-1999. Both annual values (thin line) and a 5-year smoothing function (bold line) are shown. Time periods with growth data of *S. groenlandicus* are highlighted grey, and black bars at the bottom plot denote periods with shell stable isotope (bottom bar) and trace element (top bar) results. Data from Roshydromet (Moscow, Russia).

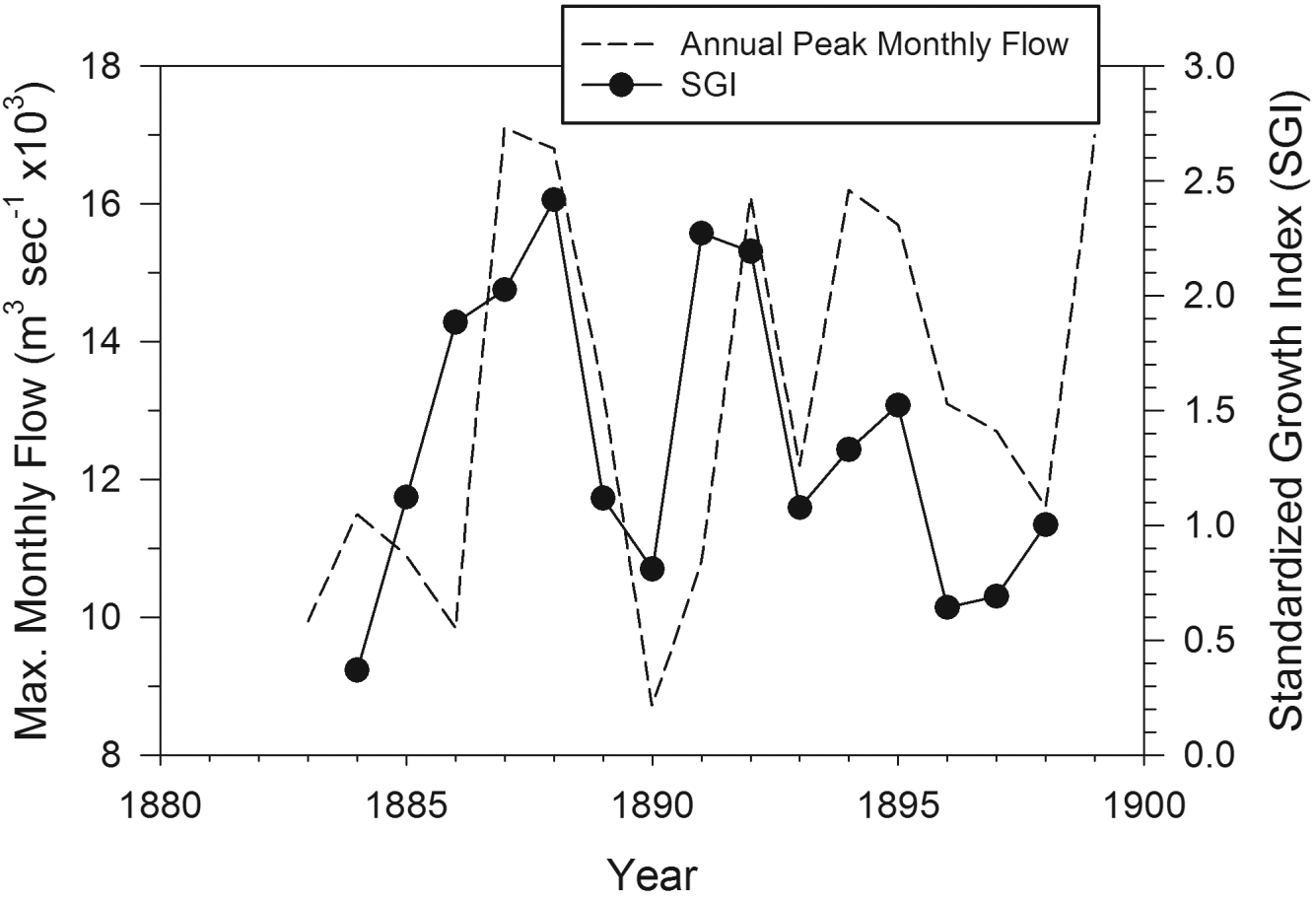

Figure 10.
Relationship between SGI of *S. groenlandicus* and maximum flow of the Severnaya Dvina River from 1884-1898.

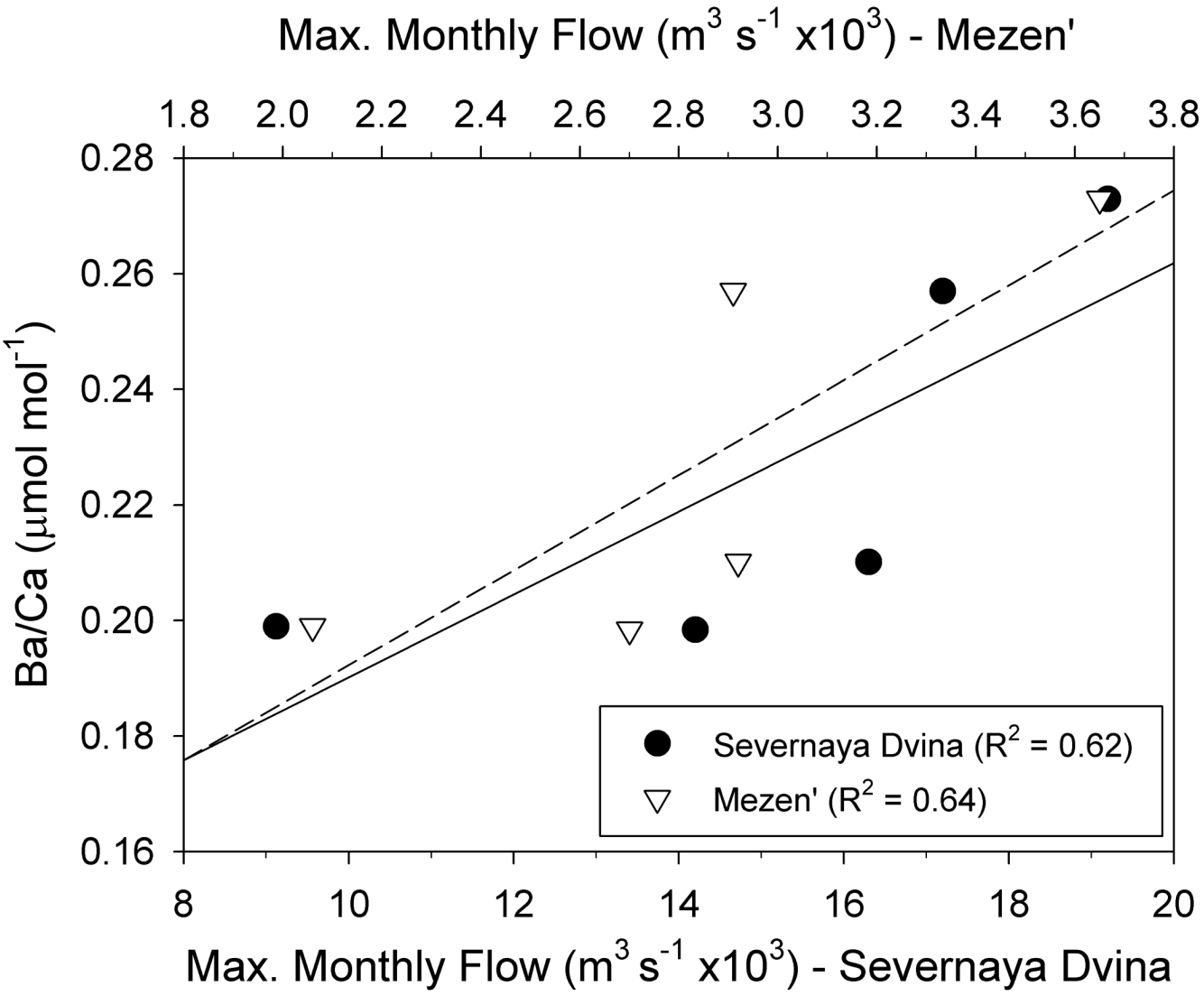

Figure 11.
Relationship between river discharge from the Severnaya Dvina and Mezen' Rivers during the month of maximum flow rate in May, and maximum annual Ba/Ca and ratios recorded in bivalve aragonite from shells collected in 1926. Lines are least squared results from linear regressions.

Table 1

Information on the samples of *Serripes groenlandicus* selected from the LMR-ZIN archive collections from the southern Barents Sea for analysis in this project.

Date Collected (YYYY.MM.DD)	Collection Number	Number Measured	Latitude	Longitude	Depth (m)	Lifespan
1899.07.18	175	4	69° 13.0′ N	36° 40.5′ E	190	1882-1899
1899.08.08	373 / 370	2	68° 51.0′ N	43° 11.3′ E	60	1884-1899
1926.07.13	480	2	68° 46.0′ N	42° 26.0′ E	78	1908-1926
1926.07.13	*156	3	68° 31.0′ N	43° 03.0′ E	59	1904-1926
1927.07.04	478	1	69° 10.0′ N	43° 13.0′ E	62	1907-1927
1927.07.09	138	1	68° 20.0′ N	41° 08.5′ E	76	1922-1927
1968.06.22	*262	1	69° 00.0′ N	45° 00.0′ E	60	1946-1968
1968.07.01	263	1	70° 30.0′ N	41° 30.0′ E	70	1948-1968

* Sampled for stable isotope and trace element ratios and isotopes (See Table 2).

Table 2

Information on *S. groenlandicus* analyzed for stable isotope and trace element ratios, the number of samples and years covered. See Figure 1 for location of samples.

Date Collected (YYYY.MM.DD)	Collection Number	Years (samples) for $\delta^{18}O$, $\delta^{13}C$	Years (samples) for trace elements
1926.07.13	156	16 (68)	6 (54)
1968.06.22	262	14 (51)	6 (51)